

Marquette University

e-Publications@Marquette

Chemistry Faculty Research and Publications

Chemistry, Department of

9-13-2018

DFT-assisted Design and Evaluation of Bifunctional Copper(I) Catalysts for the Direct Intermolecular Addition of Aldehydes and Ketones to Alkynes

Jacob D. Porter
Marquette University

Eric Greve
Marquette University

Abdulmohsen Alsafran
Marquette University

Adam R. Benoit
Marquette University

Sergey V. Lindeman
Marquette University, sergey.lindeman@marquette.edu

See next page for additional authors

Follow this and additional works at: https://epublications.marquette.edu/chem_fac

 Part of the [Chemistry Commons](#)

Recommended Citation

Porter, Jacob D.; Greve, Eric; Alsafran, Abdulmohsen; Benoit, Adam R.; Lindeman, Sergey V.; and Dockendorff, Chris, "DFT-assisted Design and Evaluation of Bifunctional Copper(I) Catalysts for the Direct Intermolecular Addition of Aldehydes and Ketones to Alkynes" (2018). *Chemistry Faculty Research and Publications*. 964.

https://epublications.marquette.edu/chem_fac/964

Authors

Jacob D. Porter, Eric Greve, Abdulmohsen Alsafran, Adam R. Benoit, Sergey V. Lindeman, and Chris Dockendorff

Marquette University

e-Publications@Marquette

Chemistry Faculty Research and Publications/College of Arts and Sciences

This paper is NOT THE PUBLISHED VERSION; but the author's final, peer-reviewed manuscript. The published version may be accessed by following the link in the citation below.

Tetrahedron, Vol. 74, No. 17 (September 13, 2018): 4823-4836. [DOI](#). This article is © Elsevier and permission has been granted for this version to appear in [e-Publications@Marquette](#). Elsevier does not grant permission for this article to be further copied/distributed or hosted elsewhere without the express permission from Elsevier.

DFT-assisted Design and Evaluation of Bifunctional Copper(I) Catalysts for the Direct Intermolecular Addition of Aldehydes and Ketones to Alkynes

Jacob D. Porter

Department of Chemistry, Marquette University, Milwaukee, WI

Eric Greve

Department of Chemistry, Marquette University, Milwaukee, WI

Abdulmohsen Alsafran

Department of Chemistry, Marquette University, Milwaukee, WI

Adam R. Benoit

Department of Chemistry, Marquette University, Milwaukee, WI

Sergey V. Lindeman

Department of Chemistry, Marquette University, Milwaukee, WI

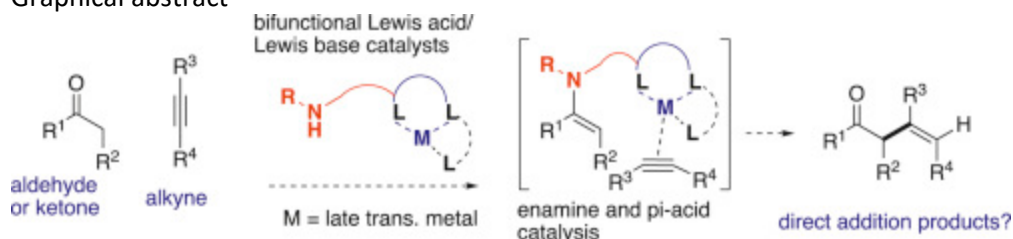
Chris Dockendorff

Department of Chemistry, Marquette University, Milwaukee, WI

Abstract

Bifunctional catalysts containing discrete metal pi-acid and amine sites were designed and investigated for the direct intermolecular addition of aldehydes and ketones to unactivated alkynes. Copper(I)-based catalysts were prioritized based on intramolecular (Conia-ene type) reactions, and complexes were designed with tridentate ligands and potentially hemilabile heterocyclic spacers. The structures of the designed catalysts were computed using density functional theory (DFT), and the relative energies of putative catalytic intermediates were estimated and used to prioritize catalyst designs. Novel bifunctional precatalysts containing a thiazole spacer were synthesized via a 9-step sequence and combined with transition metals before screening for the direct addition of aldehydes and ketones to several internal and terminal alkynes. Despite the lack of desired intermolecular reactions, DFT calculations of putative catalyst intermediates appears to be a promising strategy for the design and prioritization of bifunctional catalysts for C—C bond formation.

Graphical abstract



Keywords

Alkenylation, copper(I), Alkyne activation, Hybrid catalysis, Organocatalysis, Aldehyde, Ketone, Alkyne, DFT, Catalyst design

1. Introduction

The controlled formation of carbon–carbon bonds under mild conditions with unactivated substrates continues to be an important focus of modern organic methodology research. The identification of catalysts for such transformations has been facilitated by several enabling technologies that have flourished in recent decades, the most fundamental of which is transition metal complexes that are capable of stabilizing multiple catalytic intermediates. A complementary technology that has exploded since 2000 [1] is the use of organocatalysts for carbon–carbon bond formation [2], most commonly for the activation of aldehydes and ketones with amine-based catalysts. The use of dual organo/transition metal catalysts has further increased the range of transformations available to the organic chemist [[3], [4], [5], [6]], though a natural limitation to this approach is that separate homogeneous catalysts have the potential of poisoning each other. A related strategy is the use of multifunctional (typically bifunctional) catalysts with separate active sites positioned on a single molecule. Amino acids may be the simplest examples of bifunctional catalysts [1]; more complex examples possessing separate Lewis base and transition metal functionality have been reported [7], but have arguably not yet enabled transformations that are impossible with monofunctional or dual catalyst systems. Nonetheless, a number of promising examples have been reported over the years using bifunctional Lewis acid/Lewis base catalysts, including Ito and Hayashi's gold(I)/amino-catalyzed asymmetric isocyanoacetate aldol reaction [8], Shibasaki's aluminum(III)/phosphine oxide catalysts for asymmetric cyanosilylation of aldehydes [9], and Lectka's bifunctional cinchona alkaloid/Lewis acid catalysts for asymmetric β -lactam synthesis [10].

We hypothesize that rationally designed, bifunctional catalysts, in particular those with carefully positioned Lewis acid/Lewis base pairs, will facilitate specific bond formations not feasible using dual catalyst systems. Our first efforts in this area involved the design of bifunctional organo/transition metal catalysts for direct aldol reactions [11,12], an approach also explored in depth by Mlynarski [[13], [14], [15]] and Wang [[16], [17], [18]]. Expanding upon this approach, we endeavored to design bifunctional catalysts for direct additions of pronucleophiles, such as aldehydes and ketones, to unactivated alkenes and alkynes. *Intramolecular* direct additions of aldehydes and ketones to unactivated alkenes and alkynes have been reported; Widenhoefer has

reported palladium (II) and platinum(II)-catalyzed cyclization of alkene-tethered β -diketones [19,20], and Conia-ene type reactions with alkyne-tethered activated methylenesubstrates have been reported with a variety of transition metals [21]. Conia-ene type reactions with unactivated aldehydes and ketones are challenging, due to unfavorable equilibria with active enol nucleophiles. The use of dual amine catalysts (for aldehyde or ketone activation) and transition metal catalysts (for alkyne activation) for these intramolecular carbocyclizations has been reported by Kirsch [22], Dixon [23], Jørgensen [24], Che [25], and Michelet [[26], [27], [28], [29]].

The respective *intermolecular* direct addition reactions of aldehydes/ketones to unactivated alkenes/alkynes are rare. Widenhoefer reported the direct addition of stabilized carbon nucleophiles (1,3-dicarbonyl compounds) to ethylene and propylene using Pd(II) and Pt(II) catalysts [20]. Nakamura has also reported the metal-catalyzed addition of 1,3-dicarbonyl compounds [30] and stabilized enamines [31] to alkynes using $\text{In}(\text{OTf})_3$. Dong has reported simple bifunctional rhodium-based catalysts for the direct addition of ketones to alkenes [32], as well as enamines [33] and ketones [34] to alkynes. More commonly, such transformations are instead performed by preactivating the pronucleophile and/or the electrophile prior to a palladium- or nickel-catalyzed cross-coupling reaction between an enolate anion and an alkenyl halide to generate a β - γ unsaturated product [35]. MacMillan has also reported a dual copper(II)/amine catalyst system for the coupling of aldehydes with alkenylboronic acids under mild conditions [36].

Though attractive for their mild conditions, we hypothesized that the reported dual catalytic systems for intramolecular carbocyclizations may be unsuitable for intermolecular additions due to the fact that enamine intermediates could outcompete alkyne substrates for coordination to π -acidic metals. We reasoned that bifunctional catalysts with discrete amine and π -acidic sites could be designed that could promote net intermolecular reactions between aldehydes/ketones and alkynes via a catalytic intramolecular carbon-carbon bond formation step, with the catalyst itself bringing the reactants together to form favorable macrocyclic intermediates within the putative catalytic cycle (Fig. 1). Herein is described our early efforts towards the design, synthesis, and testing of such bifunctional catalysts for direct additions of aldehydes and ketones to unactivated alkynes.

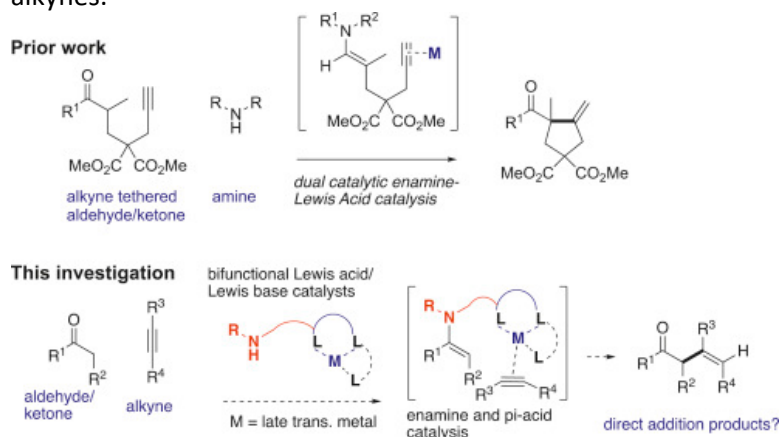


Fig. 1. Dual catalytic intramolecular (Conia-ene type) reaction (top) versus our approach to intermolecular direct additions of aldehydes/ketones to alkynes (bottom).

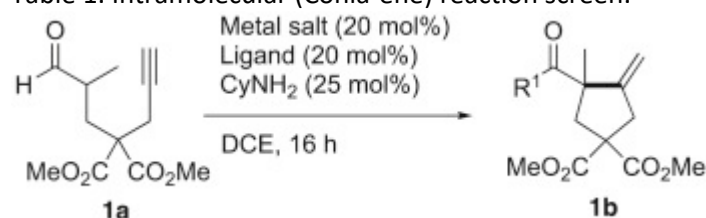
2. Results and discussion

2.1. Intramolecular (Conia-ene) reaction screening

In order to determine which metal Lewis acid and ligand combinations could be suitable for incorporation into a bifunctional catalyst, we elected to use an intramolecular reaction as a model. The formyl-alkyne substrate (**1a**) reported by Michelet [28] was used in a Conia-ene type reaction to screen a variety of metals with precedent for activating alkynes, together with cyclohexylamine as the organocatalyst for

presumed enamine generation (Table 1). The best results were obtained with the group 11 salts copper (I), silver (I), and gold (I) (entries 1, 3 and 6). With its affordability, functional group tolerance (including protic solvents), good precedent for use in Conia-ene reactions, and its compatibility with a variety of ligand types, we decided to investigate Cu(I) in greater detail. Consistent with the report from Michelet [28], we discovered that a Cu(II) source ($\text{Cu}(\text{OTf})_2$) could be conveniently used (entry 14), which we propose is reduced to an active Cu(I) species by a fraction of the enamine formed from the substrate and cyclohexylamine. We found that reactions with these Cu(II) salts tolerated a range of different ligands, including 1,3-propanediol, bipy, pyridine-2-carboxamide, 2-picolinic acid, PhBOX, and TADDOL. We were enthusiastic about identifying ligand-accelerated reactions [37], however we did not observe any substantial improvement in yield or obvious rate accelerations with different ligands relative to the unligated copper salts, though we can't rule out the possibility that the cyclohexylamine could double as a ligand for copper. The tolerance for various ligands in these Cu(I)-catalyzed reactions nonetheless prompted us to explore several heterocyclic ligand scaffolds that were already in hand for use in bifunctional catalyst systems (*vide infra*).

Table 1. Intramolecular (Conia-ene) reaction screen.



Entry	Metal catalyst	Ligand	Yield (%) ^a
1	$(\text{CH}_3\text{CN})_4\text{CuBF}_4^{\text{b}}$	–	37
2	$\text{CpCo}(\text{CO})_2^{\text{b}}$	–	–
3	$\text{PPh}_3\text{AuCl}/\text{AgSbF}_6$	–	34
4	$\text{PtCl}_2/\text{AgSbF}_6$	–	17
5	InCl_3	–	<5
6	AgSbF_6	–	52
7	$\text{Zn}(\text{OTf})_2$	–	<5
8	NiCl_2	–	<5
9	$(\text{CH}_3\text{CN})_4\text{CuBF}_4^{\text{c}}$	–	11
10	–	–	<5
11	$(\text{CH}_3\text{CN})_4\text{CuBF}_4$	H-dpa	<5
12	$(\text{CH}_3\text{CN})_4\text{CuBF}_4$	(<i>R,R</i>)-Ph-BOX	16
13	$(\text{CH}_3\text{CN})_4\text{CuBF}_4$	1,10 phenanthroline	<5
14	$\text{Cu}(\text{OTf})_2$	–	14

^a Formyl alkyne (0.020 g, 0.079 mmol) was added to a 1.5 mL HPLC vial followed by cyclohexylamine (1.8 μL , 0.016 mmol). 10 min. later, the metal salt (0.012 mmol) was added and reactions stirred for 16 h. Reaction mixtures were filtered through a silica plug, condensed, and yields measured by ^1H NMR using pentachloroethane as an internal standard.

^b Reagents were mixed in the glove box.

^c Bu_4NCl (1.0 eq) was added.

2.2. Intermolecular studies related to dual catalysis

Prior to proceeding with our strategy to build novel bifunctional catalysts, we wanted to rule out the obvious possibility of using the dual catalyst conditions for *intermolecular* reactions that were productive for intramolecular reactions. We are not aware of any reported successful nor unsuccessful attempts at such intermolecular reactions with unactivated aldehydes/ketones and alkynes using Cu(I) catalysts. We hypothesized that such reactions could be precluded by the fact that electron-rich enamine intermediates could displace the alkynes and simply act as competing ligands for the π -acid. To test this hypothesis, we performed several NMR

studies (Fig. 2). A downfield shift in the ^1H NMR signal of the alkyne proton of phenylacetylene was observed upon its addition to $(2,2'\text{-dipyridylamine})\text{CuOTf}$, from 3.07 ppm to 4.01 ppm in CDCl_3 (Fig. 2). This is consistent with formation of Cu–alkyne complex **2**; an x-ray crystal structure of the related CuBF_4 complex was obtained (Fig. 3, left). Upon addition of the enamine derived from cyclohexanone and pyrrolidine, the signal for the uncoordinated alkyne appeared at 3.07 ppm. Evidence for enamine coordination to the metal was observed as the vinyl enamine proton moves upfield from 4.29 ppm to 3.99 ppm. This chemical shift is observed with or without the presence of the alkyne, suggesting that coordination of the enamine to the metal is highly favored over alkyne coordination. The formation of 1,2-addition product **3** was subsequently observed, which presumably forms via addition of a Cu-acetylide to a transient iminium ion. Variations of this transformation, in the form of 3-component reactions (ketone, amine, and alkyne), were recently reported by Larsen [38] and Ma [39]. We also attempted stoichiometric reactions with putative internal alkyne complexes, which yielded no detectable products.

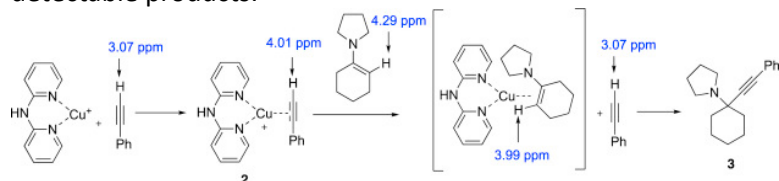


Fig. 2. Enamine displacement of alkyne from $(2,2'\text{-dipyridylamine})\text{Cu(I)}$ complex and 1,2 addition to enamine/iminium ion.

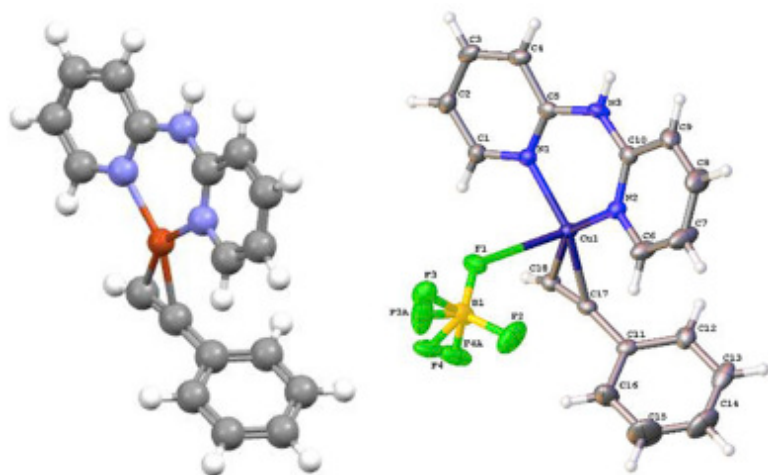


Fig. 3. X-ray structure of $(2,2'\text{-dipyridylamine})\text{Cu(I)}$ complex with phenylacetylene (left); analogous DFT-optimized structure (right).

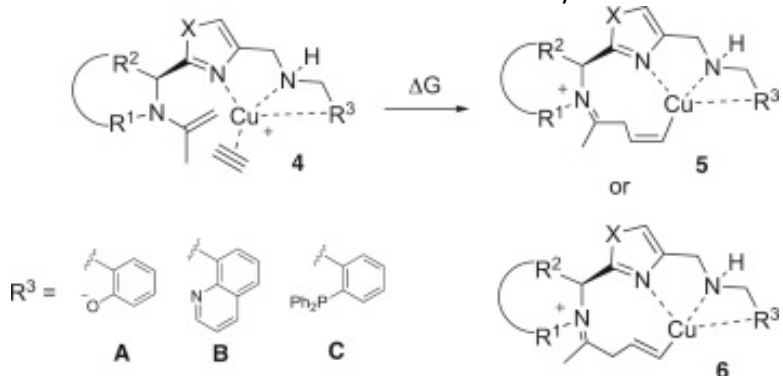
2.3. Design of bifunctional catalysts and evaluation with density functional theory (DFT) calculations

The challenge of using Cu(I) to promote intermolecular reactions with alkynes as electrophiles prompted us to start investigating the hypothesis that pseudo-intramolecular reactions promoted by a bifunctional catalyst could be productive. We elected to prioritize our ideas for novel catalysts with input from DFT geometry optimizations and energy calculations. To evaluate the feasibility of such calculations with Cu(I) complexes, we calculated the structure of the cationic version of $(2,2'\text{-dipyridylamine})\text{Cu(I)}$ using the functional B3PW91 [40], with the LANL2DZ [41] basis set for Cu, and cc-pVDZ [42] for all other atoms. The resulting minimized structure (Fig. 3, right) was in excellent agreement with the x-ray structure (Fig. 3, left), with both structures showing copper with a distorted tetrahedral coordination geometry, neglecting the BF_4 anion in the crystal structure.

Using this DFT method, we computed structures and energies of putative alkyne complexes, as well as the organocopper adducts obtained after the desired intramolecular C—C bond formation between the enamine and the alkyne. We reasoned that unfavorable energetics for this step in a catalytic cycle would make the

desired reaction unlikely, and promising catalysts will be reasonably exergonic for this step, which is depicted at the top of Table 2. The decrease in enthalpy for addition to the alkyne should outweigh the entropic costs of bringing the reacting partners together, which leads to the formation of a more constrained macrocycle. An advantage to our strategy is that the constrained approach of the enamine to the alkyne will facilitate future transition state calculations; we should emphasize that our present efforts utilize only ground state calculations of postulated catalytic intermediates.

Table 2. DFT calculations for bifunctional catalysis of C—C bond formation with acetone and acetylene^a.



Entry	R [1]	R [2]	X	R [3]	cis/trans	ΔG (kcal/mol)
1	Me	H	NH	A	cis	-0.3
2	Me	H	NH	A	trans	+1.1
3	Me	H	O	A	cis	-1.2
4	Me	H	O	A	trans	+10.3
5	Me	H	S	A	cis	-2.9
6	Me	H	S	A	trans	-0.04
7	-(CH ₂) ₃ -		S	A	cis	-2.1
8	-(CH ₂) ₃ -		S	A	trans	+11.0
9	Bn	H	S	A	cis	-3.8
10	Bn	H	S	A	trans	+3.6
11	Bn	H	S	B	cis	-10.2
12	Bn	H	S	B	trans	+6.4
13	-(CH ₂) ₃ -		S	B	cis	-5.5
14	-(CH ₂) ₃ -		S	B	trans	+1.6
15	Me	H	S	C	cis	-10.3
16	Me	H	S	C	trans	-4.1
17 ^b	Bn	H	S	B	cis	-17.1

^a All calculations used functional B3PW91, basis set LANL2DZ for copper, and basis set cc-pVDZ for all other atoms, using DCM as solvent.

^b Calculation performed with Ag(I) substituted for Cu(I).

Our initial catalyst designs are an extension of the amino acid-derived heterocyclic systems that we initially designed for asymmetric aldol reactions [11,12]. We reasoned that precatalysts with tridentate metal binding motifs would form more stable complexes with predictable coordination geometries, relative to the bidentate systems we explored previously. We also reasoned that heterocycles could act as hemilabile ligands, thus increasing flexibility during parts of the catalytic cycle and potentially permitting the relief of macrocyclic ring strain. Physical and computer models indicated that complexes with general structure **4** containing a 5-membered heterocycle (Table 2) may be able to access favorable transition state geometries for C—C bond formation, but importantly should not undergo self-quenching whereby the amine (or intermediate enamine) can coordinate (and poison) the Cu(I) in an intramolecular fashion.

The addition of the enamine to the alkyne could proceed in a *syn* or *antifashion*, to generate the organometallic adducts *cis*-(**5**) or *trans*-(**6**) (Table 2). Using acetone and acetylene as reaction partners, formation of the *cis*adducts was consistently calculated to be more exergonic than the *trans*adducts, presumably due to increased ring strain in the *trans* adducts. Assuming that both transition states are feasible, and that the difference in alternative transition state energies would be proportional to the enthalpy differences between the *cis* and *trans* adducts (Bell–Evans–Polanyi principle) [43], we would expect the *cis* adducts to form preferentially.

Variation of the heterocycle was also explored computationally. Using a glycine-derived catalyst with a phenolate as the “eastern” ligand, calculations with imidazoles, oxazoles, and thiazoles as “western” ligands were undertaken (entries 1–6). The free energy changes with the thiazoles were most favorable among these examples, with the *cis*-adduct calculated to be -2.9 kcal/mol lower in energy than the alkyne complex (entry 5). The analogous proline-derived catalyst was also computed to give the *cis*-adduct preferentially (entry 7).

Examination of the amine portion of the ligand revealed that the *N*-benzyl derived precatalyst (e.g. entry 9) was favored over the *N*-methyl or proline-derived precatalysts (entries 5, 7), with the free energy change for the formation of the *cis*-adduct calculated to be -3.8 kcal/mol (entry 9). It was hypothesized that the increased steric bulk with the *N*-benzyl substituent would also help prevent undesirable 2:1 ligand–metal complexes observed by us with other precatalysts synthesized for asymmetric aldol reactions [12]. The proline-based precatalyst was calculated to be less favorable ($\Delta G = -2.1$ kcal/mol) (entry 7), presumably due to the increased strain on the macrocyclic adduct structure from the constrained nature of the amine. The eastern portion of the precatalyst was also examined via introduction of phenolate, quinoline, and phosphine moieties (entries 9–15). Consistent with the previous trend, the *cis*-adducts of the *N*-benzyl quinoline-based precatalyst (e.g. entry 11, $\Delta G = -10.2$ kcal/mol) were calculated to be favored over the proline analogs (e.g. entry 13, -5.5 kcal/mol). Additionally, we reason that the more favorable free energy changes calculated with the quinoline- and phosphine-based catalysts is due to the increased cationic character of the metal center, relative to the phenolate complexes (e.g. entry 11 and 15 vs entry 5). The diphenylphosphine analogs (e.g. entry 15) gave similar results to the quinolines, and also provided the only favorable result for a *trans*-adduct (entry 16). Unfortunately, initial attempts to synthesize the desired phosphine-based precatalysts failed due to oxidation of the phosphine during column chromatography.

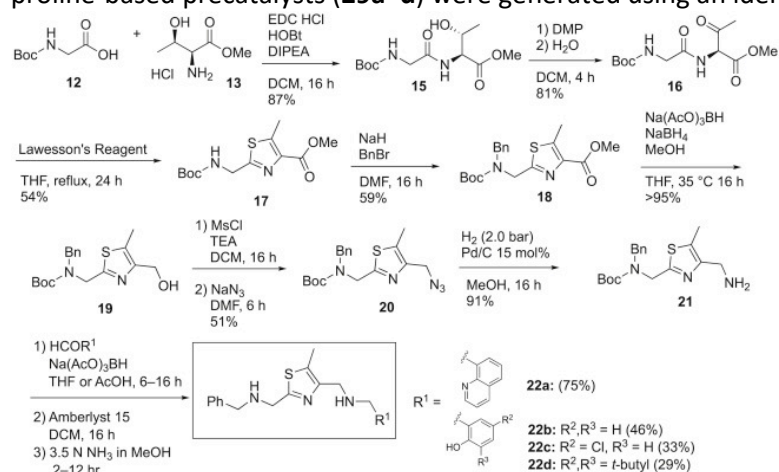
We also explored the use of Ag(I) as a metal salt (entry 17). Although formation of the C—C bond was calculated to be significantly more favorable than with the analogous Cu(I) complex (entries 11 vs 17), comparison of the orientation of the enamine to the coordinated alkyne suggested that Cu(I) could be a more suitable choice as the enamine and alkyne were perpendicular to each other in the t-shaped Ag(I) complex, and unlikely to access a reactive conformation with suitable orbital overlap (Fig. S1). However, since these were ground state calculations, and not necessarily reflective of a transition state that might or might not be accessible, we included both Cu(I) and Ag(I) in our reaction screens (vide infra).

To confirm that more complex alkynes might also be feasibly used, we performed DFT calculations using 1-butyne as an acceptor (Table S1). The results with acetone and 1-butyne predict thermodynamically favorable adduct formations. Calculations were run for the *cis*-adduct only for these substrates for comparative purposes given the trend observed in Table 2 showing the *trans*-adduct to be less favorable in almost all cases. Addition to the terminal carbon of the alkyne (giving adduct **8**) or internal carbon (giving **9**) was compared with two quinoline-based complexes (Table S1), and the addition to the terminal alkyne carbon was predicted to be more favorable with both. In addition to favorable thermodynamic transformation from enamine complex to adduct, we also wished to examine the distance and orientation of the enamine with respect to the alkyne in the alkyne complex (e.g. **10**, Fig. S2). Even though we did not attempt to determine transition state structures, it appears that the enamine and alkyne could adopt suitable positions for productive reactions. In adduct complexes such

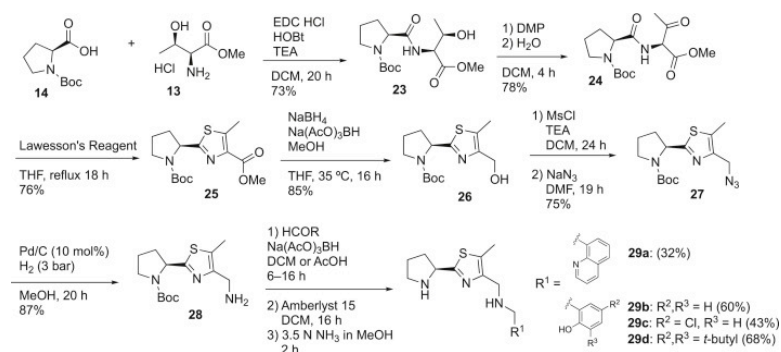
as **11**, we commonly observed de-coordination of the thiazole nitrogen from the metal center. The hemilabile nature of this coordination may allow the adduct to adopt a macrocyclic species with reduced strain.

2.4. Synthesis of precatalysts

Our next objective was to develop modular syntheses of desirable heterocyclic precatalysts. Our results are summarized in Scheme 1, Scheme 2. Based on our DFT calculations, we focused on thiazole-containing precatalysts, initially using *N*-Boc glycine (**12**) as starting material (Scheme 1). Amide coupling with threonine methyl ester **13**, followed by Dess-Martin Periodinane (DMP) oxidation, yielded the known dipeptidyl ketone **16** in good yield. Heating with Lawesson's reagent provided the thiazole **17**[44], followed by *N*-benzylation using sodium hydride and benzyl bromide in DMF to give **18**. Reduction of the ester proceeded cleanly with sodium borohydride and catalytic sodium triacetoxyborohydride. Mesylation of the primary alcohol (**19**) and addition of sodium azide generated azide **20**, which was reduced with hydrogen and catalytic palladium on carbon. The resulting primary amine **21** could be combined in a modular fashion using reductive alkylation (amination) conditions with a variety of aldehydes to generate final precatalysts (**22a–d**) after Boc removal. Reductive amination of the quinoline-based precatalysts in THF was complicated by the prominent formation of bis-alkylated byproducts which were not easily separable by column chromatography. Stepwise attempts to reduce the pre-formed imine with sodium borohydride yielded identical results. The use of acetic acid as a solvent was discovered to suppress the formation of the overalkylated byproduct, though reactions with these substrates were difficult to push to completion. A sulfonic acid resin (Amberlyst 15[®]) was effective for both Boc removal and trapping the final diamine products, which allowed impurities to be washed away and the desired products released in high purity after basification with ammonia in methanol. Analogous proline-based precatalysts (**29a–d**) were generated using an identical strategy, with similar results (Scheme 2).



Scheme 1. Synthesis of glycine-based precatalysts.

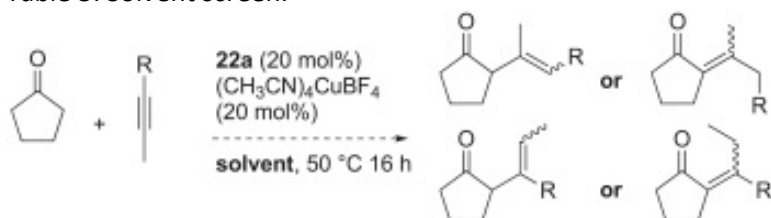


Scheme 2. Synthesis of proline-based precatalysts.

2.5. Reaction screening

With a focused library of precatalysts in hand, we proceeded to test them in a variety of reaction screens, utilizing GC-MS to analyze each reaction. For initial screening, cyclopentanone was selected due to its well-established reactivity for enamine formation [45,46]. Internal alkynes were chosen as initial substrates due to the possibility that terminal alkynes may form undesired copper-acetylide species. Results from a representative solvent screen with precatalyst **22a** are given in Table 3. Polar solvents (entries 1–6) yielded no reaction at 50 °C. It is plausible that the coordinating nature of these solvents prevented interaction of the metal salt with the substrates. Chloroform and toluene (entries 7–10) also showed only starting material after reaction at 50 °C. Nitromethane and THF (entries 13–16) produced an unknown, undesired byproduct that was also present in a control reaction run in THF where the hexyne had been omitted (entry 17). DCE and dioxane (entries 18–21) led to consumption of cyclopentanone, but gave complex, intractable mixtures of products. Given the use of DCE in the analogous intramolecular carbocyclization reactions, we explored additional substrates in this solvent with our library of precatalysts (Table 4). This screening showed that phenol based precatalysts (**22b–d** and **29b–d**) were inactive under the reaction conditions. Quinoline-based precatalysts (**22a** and **29a**) showed complex mixtures of products. Analysis of these mixtures showed that GC-MS peaks were common amongst reactions with shared substrates. For example, reactions with acetone (Table 4, entries 1–5) contained a similar mixture of common byproducts. Similarly, reactions with 2-hexyne (entries 4, 9, 14, 19) also yielded a set of common byproducts that did not correspond to any desired products nor their derivatives, such as multiple alkenylation products, as determined by GC-MS and NMR of scaled up reactions. No GC-MS peaks were identified that were unique to a specific set of substrates, which would have suggested a unique and potentially desirable reaction. Based on the GC-MS data, we believe that the products formed under these conditions are primarily due to carbonyl-carbonyl or alkyne-alkyne coupling reactions. GC-MS evidence for aldol self-condensation products was observed in some cases, most notably when phenylacetaldehyde was used as the carbonyl compound (entries 11–15). A second prominent byproduct seen via GC-MS for samples that contained phenylacetylene (entries 1, 6, 11, 16) was 1,4-diphenylbutadiyne. The presence of this byproduct in these samples was confirmed by comparison of the GC-MS traces to that of a commercial sample of 1,4-diphenylbutadiyne. Additionally, select reactions were run with AgBF_4 as the metal salt instead of $(\text{CH}_3\text{CN})_4\text{CuBF}_4$ (entries 21–26), under the conditions of Table 4. No reactions were observed in any of these cases.

Table 3. Solvent screen.



Entry ^a	Solvent	R	Result ^b
1	DMSO ^d	Ph	A
2	DMSO ^d	(CH ₂) ₂ Me	A
3	DMF ^d	Ph	A
4	DMF ^d	(CH ₂) ₂ Me	A
5	acetonitrile	Ph	A
6	acetonitrile	(CH ₂) ₂ Me	A
7	chloroform	Ph	A
8	chloroform	(CH ₂) ₂ Me	A
9	toluene	Ph	A
10	toluene	(CH ₂) ₂ Me	A
11	MeOH	Ph	A
12	MeOH	(CH ₂) ₂ Me	A

13	nitromethane ^c	Ph	C
14	nitromethane ^c	(CH ₂) ₂ Me	C
15	THF	Ph	C
16	THF	(CH ₂) ₂ Me	C
17	THF	no alkyne	C
18	dioxane	Ph	B
19	dioxane	(CH ₂) ₂ Me	B
20	DCE	Ph	B
21	DCE	(CH ₂) ₂ Me	B

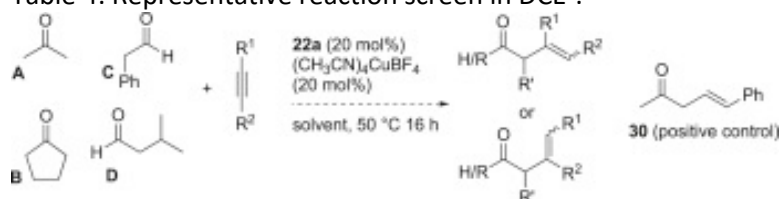
^a In a glovebox, precatalyst **22a** (2 mg, 0.005 mmol) was dissolved in DCE (0.5 mL) and added to (CH₃CN)₄CuBF₄ (0.005 mmol) in a 1.5 mL HPLC vial. The alkyne (0.130 mmol) and carbonyl compound (0.026 mmol) were added as solutions in DCE (0.150 and 0.100 mL, respectively). The vials were removed from the glovebox and shaken at 50 °C for 16 h. Crude reaction mixtures were condensed and analyzed directly by GC-MS.

^b Results: A: No reaction; B: complex mixture; C: carbonyl-derived byproducts observed, as determined by a control reaction without the alkyne.

^c Reaction heated to 95 °C.

^d Samples were diluted with 5 mL water and extracted with ether (3 × 2 mL), before being condensed and analyzed by GC-MS.

Table 4. Representative reaction screen in DCE^a.



Entry ^a	Aldehyde/ketone	R [1]	R [2]	Result ^b
1	A	H	Ph	A, B, C
2	A	Me	Ph	B
3	A	H	(CH ₂) ₂ Me	B
4	A	Me	(CH ₂) ₂ Me	B
5	A	H	TMS	B
6	B	H	Ph	A, B, C
7	B	Me	Ph	B
8	B	H	(CH ₂) ₂ Me	B
9	B	Me	(CH ₂) ₂ Me	B
10	B	H	TMS	B
11	C	H	Ph	A, B, C
12	C	Me	Ph	B
13	C	H	(CH ₂) ₂ Me	B
14	C	Me	(CH ₂) ₂ Me	B
15	C	H	TMS	B
16	D	H	Ph	A, B, C
17	D	Me	Ph	B, C
18	D	H	(CH ₂) ₂ Me	B, C
19	D	Me	(CH ₂) ₂ Me	B, C
20	D	H	TMS	B, C
21 ^c	A	H	(CH ₂) ₂ Me	D
22 ^c	A	Me	(CH ₂) ₂ Me	D

23 ^c	B	H	(CH ₂) ₂ Me	D
24 ^c	B	Me	(CH ₂) ₂ Me	D
25 ^c	C	H	(CH ₂) ₂ Me	D
26 ^c	C	Me	(CH ₂) ₂ Me	D

^a In a glovebox, precatalyst **22a** (2 mg, 0.005 mmol) was dissolved in DCE (0.5 mL) and added to (CH₃CN)₄CuBF₄ (0.005 mmol) in a 1.5 mL HPLC vial. The alkyne (0.130 mmol) and carbonyl compound (0.026 mmol) were added as solutions in DCE (0.150 and 0.100 mL, respectively). The vials were removed from the glovebox and shaken at 50 °C for 16 h. Crude reaction mixtures were analyzed directly by GC-MS.

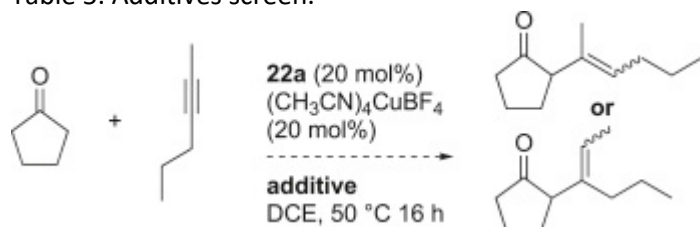
^b Results: A: dimerization of alkyne; B: complex mixture; C: carbonyl-derived byproducts observed, as determined by a control reaction without the alkyne. D: no reaction.

^c Reaction run with AgBF₄ instead of (CH₃CN)₄CuBF₄.

To ensure that we could detect desired product formation, a control reaction was run to confirm that trace amounts of desired product could be detected in our crude reaction mixtures via GC-MS. An authentic sample for the addition of acetone to phenylacetylene (**30**) was synthesized according to a protocol reported by Trofimov [47]. Two parallel reactions were set up containing acetone and phenylacetylene substrates (Table 4, entry 1), and one reaction was doped with the positive control (**30**) at 5 mol%. After stirring at 50 °C for 24 h, both reactions were analyzed via GC-MS. The positive control was detected in the reaction that was doped and it was not detected in the undoped reaction.

A range of acidic additives were additionally tested for the addition of cyclopentanone to 2-hexyne, along with the non-coordinating base 2,6-di-*tert*-butylpyridine (Table 5). No reactions were observed in any cases that previously led to consumption of substrates, such as the control reaction with no additive (entry 7).

Table 5. Additives screen.



Entry ^a	Additive	Result ^b
1	4-nitrophenol	A
2	benzoic acid	A
3	<i>p</i> -TsOH	A
4	acetic acid	A
5	TFA	A
6	2,6-Di- <i>tert</i> -butylpyridine	A
7	–	B

^a In a glovebox, precatalyst **22a** (2 mg, 0.005 mmol) was dissolved in DCE (0.5 mL) and added to (CH₃CN)₄CuBF₄ (0.005 mmol) in a 1.5 mL HPLC vial. The alkyne (0.130 mmol) and carbonyl compound (0.026 mmol) were added as solutions in DCE (0.150 and 0.100 mL, respectively). Next, additives (0.005 mmol) were added as solutions in DCE (0.100 mL). The vials were removed from the glovebox and shaken at 50 °C for 16 h. Crude reaction mixtures were condensed and analyzed directly by GC-MS.

^b Results: A: No reaction; B: complex mixture.

2.6. X-ray crystal and NMR studies

Concurrent with our efforts to screen catalysts and reaction conditions, we attempted to obtain single crystals of various Cu(I) complexes to corroborate our DFT studies. It was necessary to develop a protocol to cope with the

additional challenge of keeping oxygen sensitive Cu(I) complexes in an inert atmosphere throughout the course of the crystallization (see Experimental Section). Unfortunately, attempts to obtain single crystals of Cu(I) complexes with our precatalysts have been unsuccessful. Crystallization trials were run with all precatalysts, however efforts focused mainly on **22a**, **29a**, and **29d**, particularly because **22a** and **29a** showed the greatest apparent reactivity in reaction screens. Due to its polar, non-coordinating nature, nitromethane was chosen as the strong solvent and ultimately a 1:1 nitromethane: benzene mixture was chosen as the strong solvent with ether or pentane as the weak solvent. Samples containing phenol-based precatalysts **22b–d** and **29b–d** led to the formation of $(\text{CH}_3\text{CN})_4\text{CuBF}_4$ crystals in 1:1 nitromethane: benzene with either ether or pentane as the weak solvent. This observation suggests that ligand affinity for Cu(I) may not be as high as anticipated. Deprotonation of precatalysts **22d** and **29d** using NaH prior to complexation of $(\text{CH}_3\text{CN})_4\text{CuBF}_4$ yielded similar results. However, $(\text{CH}_3\text{CN})_4\text{CuBF}_4$ crystals were not observed in samples containing the quinoline-based precatalysts. In these cases, oiling out of the precatalyst was observed. Exploration of a range of Cu(I) salts as well as Zn(II), Ag(I), and In(III) salts with **22a** eventually yielded a Ag(I) crystal with a 2:2 ligand to metal stoichiometry (Fig. 4). Both ligands are bridging the Ag(I) ions, which are non-equivalent. Ag1 has a linear geometry via coordination from the *N*-benzyl N4 and secondary N6 amino groups from two different ligands, but the complex could also be described as having a seesaw geometry with additional coordination possible from quinoline N5 and thiazole N3. Ag2 has a distorted trigonal planar coordination geometry (chelated by thiazole N7, secondary amine N8, and *N*-benzyl N2). It is also disordered in the structure, present in two different positions due to pyramidal inversion of the benzylamine nitrogen (N8). Of special note is that neither of the metals are coordinated to all three of the desired coordinating groups of the precatalyst, namely the quinoline, thiazole, and the secondary amine proximal to the quinoline. Coordination of the *N*-benzylamine (required as an aminocatalyst), instead of the quinoline, as observed in the bimetallic structure in Fig. 4, could provide an explanation for the lack of activity of this catalyst class.

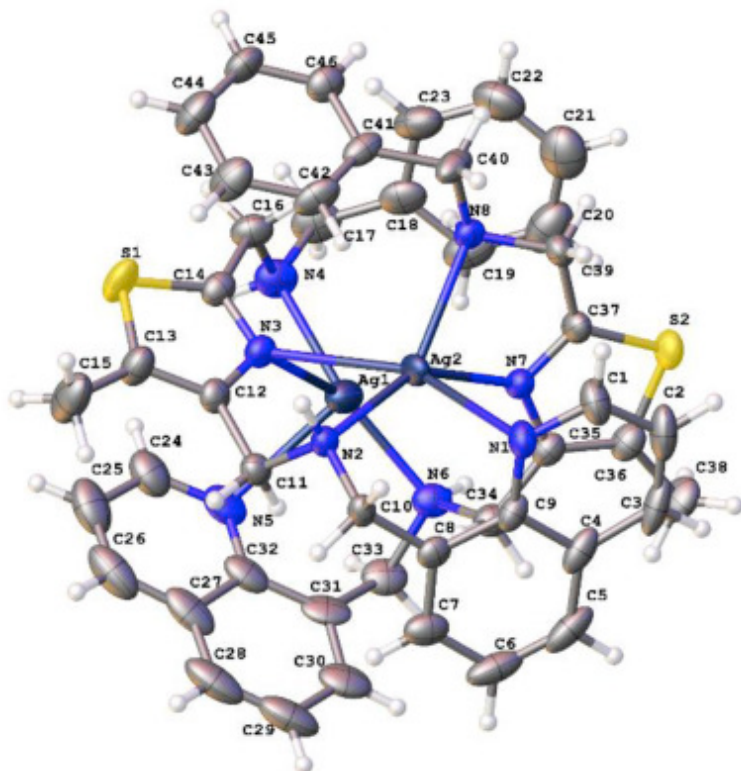


Fig. 4. X-ray structure of 2:2 complex of **22a** and AgBF_4 .

The lack of a single, well-defined catalyst complex, as well as undesired coordination of the organocatalytic amine to metal centers, is also consistent with ^1H NMR experiments. Addition of $(\text{CH}_3\text{CN})_4\text{CuBF}_4$ to bifunctional precatalyst **22a** in CD_3NO_2 , with the sample prepared in the glovebox to inhibit Cu(II) formation, showed

significant broadening of the ligand peaks with subtle chemical shift changes in the quinoline proton signals of roughly 0.1 ppm (see Supporting Information, Fig. S3). Addition of phenylacetylene further broadened the ligand peaks almost completely into the baseline with a minor additional downfield shift of the most downfield quinoline proton. The acetylene proton was also slightly shifted from its original position, however it is unknown if this shift is due to interaction with ligand-bound or free copper (I). Broadening of the ligand (precatalyst) peaks upon addition of the metal is indicative of a slow exchange (on the NMR timescale) between different complexes. The lack of discrete and characterizable Cu(I) complexes may be due to diverse coordination complexes that may be facilitated by the organocatalytic amine. We hypothesize that alternative coordination geometries, in particular hindered square planar complexes, may be more suitable for promoting intermolecular direct additions to alkynes.

3. Conclusions

We have investigated a strategy for the design and prioritization of potential bifunctional catalysts using as a guide DFT calculations of putative catalytic intermediates before and after C—C bond formation. This strategy was applied for the first time to novel Cu(I) complexes containing tridentate, heterocyclic ligands. We conclude that the designed bifunctional systems may not have sufficient affinity for Cu(I), or may undergo a range of dynamic coordination modes that precludes the formation of effective catalysts or well-characterizable complexes suitable for the desired direct additions of aldehydes and ketones to alkynes. Studies continue in our laboratories using alternative scaffolds with significantly greater rigidity.

4. Experimental section

4.1. General information: DFT calculations

Starting points for enamine–alkyne complex calculations were set by starting with the enamine–Cu(I)–acetylene complex (before C—C bond formation) and adduct (after C—C bond formation) from Table 2, entry 5. These complexes were drawn within the Avogadro [48] molecular visualization program and subjected to preliminary optimization with molecular mechanics. The alkyne and enamine carbons were fixed at a specific orientation and distance while the rest of the molecule was optimized using the auto-optimization feature (force field set to UFF, 4 steps per update, and steepest descent algorithm). The resulting coordinates were added to the Gaussian 09 input file for DFT calculations. Subsequent calculations of different precatalysts/substrates were preoptimized in Avogadro as described above, while keeping the enamine-alkyne starting orientation and distance from the original calculation constant. Starting adduct complexes were preoptimized using molecular mechanics as described above.

Geometries were then optimized and energies were calculated by DFT using the B3PW91 functional and the basis sets LANL2DZ for all metals and cc-pVDZ for other atoms, using the PCM solvation model with dichloromethane. Enthalpies and free energies were calculated at 298.15 K using unscaled harmonic vibrational frequencies. All calculations were performed with Gaussian 09 on the Père cluster at Marquette University.

4.2. General information: synthesis

A Vacuum Atmospheres Co. Omni-Lab glovebox was used for weighing out air sensitive materials, as noted in the detailed protocols. All reactions utilized magnetic stirring unless otherwise noted.

All reagents and solvents were purchased from commercial vendors and used as received. NMR spectra were recorded on Varian 300 MHz or 400 MHz spectrometers as indicated. Proton and carbon chemical shifts are reported in parts per million (ppm; δ) relative to tetramethylsilane, CDCl₃, or DMSO-*d*₆ (¹H δ 0, ¹³C δ 77.16, or ¹³C δ 39.5, respectively). NMR data are reported as follows: chemical shifts, multiplicity (obs = obscured,

app = apparent, br = broad, s = singlet, d = doublet, t = triplet, q = quartet, sxt = sextet, m = multiplet, comp = complex overlapping signals); coupling constant(s) in Hz; integration. Unless otherwise indicated, NMR data were collected at 25 °C. Flash chromatography was performed using Biotage SNAP cartridges filled with 40–60 µm silica gel, or C18 reverse phase columns (Biotage® SNAP Ultra C18 or Isco Rediseq® Gold C18Aq) on Biotage Isolera systems, with photodiode array UV detectors. Analytical thin layer chromatography (TLC) was performed on Agela Technologies glass plates with 0.25 mm silica gel with F254 indicator. Visualization was accomplished with UV light (254 nm) and aqueous potassium permanganate (KMnO₄) stain followed by heating, unless otherwise noted. Tandem liquid chromatography/mass spectrometry (LC-MS) was performed on a Shimadzu LCMS-2020 with autosampler, photodiode array detector, and single-quadrupole MS with ESI and APCI dual ionization, using a Peak Scientific nitrogen generator. Unless otherwise noted, a standard LC-MS method was used to analyze reactions and reaction products: Phenomenex Gemini C18 column (100 × 4.6 mm, 3 µm particle size, 110 Å pore size); column temperature 40 °C; 5 µL of sample in MeOH or CH₃CN at a nominal concentration of 1 mg/mL was injected, and peaks were eluted with a gradient of 25–95% CH₃CN/H₂O (both with 0.1% formic acid) over 5 min, then 95% CH₃CN/H₂O for 2 min. Purity was measured by UV absorbance at 210 or 254 nm. High-resolution mass spectra were obtained at the University of Wisconsin-Milwaukee Mass Spectrometry Laboratory with a Shimadzu LCMS-IT-TOF with ESI and APCI ionization. Gas chromatography/mass spectrometry (GC-MS) was performed with Agilent Technologies 6850 GC with 5973 MS detector, and Agilent HP-5S or Phenomenex Zebron ZB-5MSi Guardian columns (30 m, 0.25 mm ID, 0.25 µm film thickness). Preparative HPLC was performed on a Shimadzu LC-20AP preparative HPLC with autosampler, dual wavelength detector, and fraction collector. Method: Column: Phenomenex Gemini C₁₈ semi-preparative (250 × 10 mm, 5 µm particle size, 110 Å pore size); Mobile Phase: Solvent A: H₂O w/0.1% formic acid; Solvent B: MeOH w/0.1% formic acid; Peak collection: measured by UV absorbance at 210 or 254 nm; Sample Injection: 0.3 mL (2 mL sample loop) of sample in DMSO; Flow Rate: 6.0 mL/min; Gradient: 0–1.5 min: 25% MeOH, 1.5 min–12 min: 25%–95% MeOH, 12 min–19 min: 95% MeOH. IR spectra were obtained as a thin film on ZnSe plate using a Thermo Scientific Nicolet iS5 spectrometer. Optical rotations were measured with a Rudolph Research Analytical Autopol polarimeter at λ = 589 nm, using a 2 mL cell with 10 cm path length. Specific rotations are reported as follows: [α]_D^T (c = g/100 mL, solvent). A VWR® Analog vortex mixer fitted with a 5 × 5" sample box with divider was used to shake reaction samples.

Alkyne and carbonyl stock solutions used for screening were made outside of the glovebox and purged with argon for 10 min before being brought into the glovebox for use. Ligand solutions for crystallizations of Cu(I) complexes were made on the benchtop and purged with argon for 10 min before being brought into the glovebox for use.

4.3. Synthesis of precatalysts

4.3.1. Methyl (2*S*,3*R*)-2-(2-((*tert*-butoxy)carbonyl)amino)acetamido)-3-hydroxybutanoate (**15**)
N-Boc glycine (**12**) (6.28 g, 35.9 mmol) and *L*-threonine methyl ester, HCl salt (**13**) (6.08 g, 35.9 mmol) were added to a 500 mL round bottom flask with stir bar and dissolved with DCM (250 mL). HOBt (6.04 g, 39.4 mmol) was added followed by DIPEA (15.6 mL, 89.6 mmol), and sealed with a septum. The reaction stirred for 3 min until the solids dissolved, then EDC HCl (7.56 g, 39.4 mmol) was added. The reaction stirred for 16 h. A sample aliquot was taken from the reaction, dissolved in 1 mL HPLC grade MeCN, and analyzed with LCMS to confirm reaction completion. The reaction was washed with half saturated sodium bicarbonate (2 × 250 mL), and 0.1 N HCl (2 × 250 mL). The combined aqueous washes were saturated with NaCl and extracted with EtOAc (3 × 250 mL). The combined organics were washed with brine dried over sodium sulfate, filtered, and condensed to give the title compound as a clear oil (8.00 g, 77%). The crude product was pushed forward without further purification. This compound has been previously reported and characterized (CAS# 67864-88-4). ¹H NMR (400 MHz, CDCl₃) δ = 1.20 (d, *J* = 8.2 Hz, 3 H), 1.45 (s, 9 H), 3.75 (s, 3 H), 3.88 (br s, 2 H), 4.34 (br s, 1 H), 4.58 (d, *J* = 8.6 Hz, 1 H), 5.72 (br s, 1 H), 7.26 (d, *J* = 8.2 Hz, 1 H).

4.3.2. Methyl (2S)-2-(2-(((*tert*-butoxy)carbonyl)amino)acetamido)-3-oxobutanoate (16)

Alcohol **15** (7.20 g, 24.9 mmol) was added to a 1 L round bottom flask with stir bar followed by DCM (600 mL) and Dess-Martin periodinane (12.62 g, 29.8 mmol). The flask was sealed with a septum and purged with nitrogen. The reaction was stirred for 1.5 h before water (0.45 mL, 24.8 mmol) was added, and the reaction stirred for another 3 h. A sample aliquot was taken from the reaction, dissolved in 1 mL HPLC grade MeCN, and analyzed with LC-MS to confirm reaction completion. The reaction was poured on to a 10% sodium thiosulfate solution (400 mL) and stirred for 20 min. The organic layer was separated, washed with saturated aq. sodium bicarbonate (2 × 250 mL) and brine, then dried over sodium sulfate, filtered, and condensed to give the title compound as a yellow oil (5.80 g, 81%). The crude product was pushed forward without further purification. This compound has been previously reported and characterized (CAS# 1166831-50-0).

4.3.3. Methyl 2-(((*tert*-butoxy)carbonyl)amino)methyl)-5-methyl-1,3-thiazole-4-carboxylate (17)

Ketone **16** (5.84 g, 20.3 mmol) was added to a 250 mL round bottom flask with stir bar followed by anhydrous THF (150 mL) under a nitrogen atmosphere. Lawesson's Reagent (12.29 g, 30.4 mmol) was added and the flask was fitted with a reflux condenser before the apparatus was sealed with a septum and purged with nitrogen for 15 min, before being heated to reflux for 16 h. A sample aliquot was taken from the reaction, dissolved in 1 mL HPLC grade MeCN, and analyzed with LC-MS to confirm reaction completion. The reaction was condensed to an oil, then dissolved in EtOAc (250 mL) and washed with saturated sodium bicarbonate (2 × 250 mL). The aqueous washes were extracted with EtOAc (100 mL), and the combined organics were washed with brine and condensed to a yellow oil. The oil was adsorbed onto SiO₂ (25 g), then purified by flash chromatography (100 g SiO₂ cartridge; 0–100% EtOAc/hexanes gradient) to yield the title compound as a yellow oil (3.12 g, 53%). This compound has been previously reported and characterized (CAS# 232280-95-4). ¹H NMR (400 MHz, CDCl₃) δ = 1.47 (s, 9 H), 2.74 (s, 3 H), 3.92 (s, 3 H), 4.55 (s, 2 H), 5.47 (br s, 1 H).

4.3.4. Methyl 2-({benzyl}(((*tert*-butoxy)carbonyl)amino)methyl)-5-methyl-1,3-thiazole-4-carboxylate (18)

Carbamate **17** (3.00 g, 10.5 mmol) was added to an oven dried 250 mL round bottom flask with stir bar containing 4 Å molecular sieves (1.0 g). The flask was sealed with a septum and flushed with nitrogen, then anhydrous DMF (75 mL) was added. After 1 h the DMF solution was syringed away from the sieves into a second 250 mL oven round bottom flask with stir bar sealed under nitrogen. The sieves were rinsed with DMF under nitrogen (1 × 10 mL). Benzyl bromide (1.65 mL, 9.63 mmol) was added via syringe followed by NaH (0.545 g, 13.6 mmol). The reaction was stirred for 16 h under nitrogen. A sample aliquot was taken from the reaction, dissolved in 1 mL HPLC grade MeCN, and analyzed with LC-MS to confirm reaction completion. The reaction was diluted with ether (250 mL), quenched with saturated aqueous ammonium chloride (150 mL), then diluted with water (750 mL). The organic layer was separated and the aqueous layer was saturated with solid NaCl, then extracted with ether (2 × 75 mL). The combined organics were washed with brine, dried over sodium sulfate, filtered, and condensed to afford a light brown oil. The crude was purified by flash chromatography (50 g SiO₂ cartridge; 0–45% EtOAc/hexanes gradient) to give the title compound as a yellow oil (2.30 g, 58%). TLC R_f = 0.33 (70:30 hexane:EtOAc); ¹H NMR (300 MHz, CDCl₃) δ = 1.33–1.73 (m, 9 H), 1.51 (s, 9 H), 2.75 (s, 3 H), 3.93 (s, 3 H), 4.48 (s, 2 H), 4.63 (d, *J* = 1.0 Hz, 2 H), 7.28 (t, *J* = 8.8 Hz, 5 H); ¹³C NMR is complicated due to rotamers. ¹³C NMR (75 MHz, CDCl₃) δ = 13.4, 28.6, 48.4, 50.3, 51.1, 52.3, 81.3, 127.7, 128.4, 128.8, 137.5, 140.5, 145.9, 146.5, 155.2, 155.8, 163.0, 164.9, 165.5; IR (film) 2972, 1696, 1157, 700 cm⁻¹; HRMS (ESI⁺) calculated for C₁₉H₂₄N₂O₄S [M+H] 377.1535, found 377.1497.

4.3.5. *Tert*-butyl *N*-benzyl-*N*-{[4-(hydroxymethyl)-5-methyl-1,3-thiazol-2-yl]methyl}carbamate (19)

Ester **18** (2.00 g, 5.31 mmol) was added to an oven dried 100 mL round bottom flask with stir bar followed by sodium triacetoxyborohydride (0.059 g, 0.27 mmol), and sodium borohydride (0.433 g, 11.2 mmol). The flask was sealed with a septum and purged with nitrogen before anhydrous THF (30 mL) was added via cannula. The reaction was stirred for 5 min, then anhydrous methanol (0.86 mL, 21.3 mmol) was added via syringe over 5 min. The reaction was heated at 35 °C for 16 h. A sample aliquot was taken from the reaction, dissolved in

1 mL HPLC grade MeCN, and analyzed with LC-MS to confirm reaction completion. The reaction was diluted with EtOAc (50 mL) and quenched with saturated aqueous ammonium chloride. The layers were separated and the aqueous layer was saturated with solid NaCl, then extracted with 10% MeOH in DCM (3 × 75 mL). The combined organics were washed with brine and condensed to give the title compound as a yellow oil (1.93 g, 104%). The crude material was moved forward without purification. TLC R_f = 0.31 (50:50 hexane:EtOAc); ^1H NMR (300 MHz, CDCl_3) δ = 1.48 (br s, 9 H), 2.36 (br s, 3 H), 4.27–4.83 (m, 6 H), 7.26 (s, 5 H); ^{13}C NMR is complicated due to rotamers. ^{13}C NMR (75 MHz, CDCl_3) δ = 11.2, 28.6, 47.7, 47.9, 50.1, 50.8, 58.0, 77.5, 81.1, 127.6, 127.8, 128.4, 128.7, 130.1, 130.4, 137.7, 137.9, 150.7, 155.3, 155.7, 165.1, 165.5; IR (film) 3439, 1683, 1495, 1407, 700 cm^{-1} ; HRMS (ESI⁺) calculated for $\text{C}_{18}\text{H}_{25}\text{N}_2\text{O}_3\text{S}$ [M+H] 349.1586, found 349.1547.

4.3.6. *Tert*-butyl *N*-{[4-(azidomethyl)-5-methyl-1,3-thiazol-2-yl]methyl}-*N*-benzylcarbamate (20)

Alcohol **19** (1.90 g, 5.45 mmol) was added to an oven dried 50 mL round bottom flask with stir bar. The flask was sealed under nitrogen and anhydrous DCM (30 mL) was added followed by mesyl chloride (0.63 mL, 8.18 mmol) and triethylamine (1.14 mL, 8.18 mmol). The reaction was warmed to 30 °C and stirred for 12 h. The DCM was removed via rotary evaporator, and the crude oil was taken up into anhydrous DMF (30 mL). Sodium azide (0.425 g, 6.54 mmol) was added in one portion and the reaction stirred for 6 h. A sample aliquot was taken from the reaction, dissolved in 1 mL HPLC grade MeCN, and analyzed with LC-MS to confirm reaction completion. The reaction was diluted with ether (250 mL) and water (750 mL), and the organic layer was separated and the aqueous layer extracted with ether (2 × 100 mL). The combined organics were washed with brine, dried over sodium sulfate, filtered, and condensed to give a brown oil. The oil was dissolved with minimal DCM and purified by flash chromatography (25 g SiO_2 cartridge; 0–22% EtOAc:hexanes gradient) to give the title compound as a yellow oil (2.20 g, 51%). TLC R_f = 0.47 (80:20 hexane:EtOAc); ^1H NMR (300 MHz, CDCl_3) δ = 1.48 (s, 9 H), 2.43 (s, 3 H), 4.33 (s, 2 H), 4.41–4.67 (m, 4 H), 7.16–7.40 (m, 5 H). ^{13}C NMR is complicated due to rotamers. ^{13}C NMR (75 MHz, CDCl_3) δ = 11.5, 28.6, 47.6, 47.9, 50.0, 50.7, 77.5, 81.1, 127.7, 127.9, 128.5, 128.8, 132.3, 132.7, 137.6, 137.7, 145.8, 155.3, 155.7, 165.1, 165.5; IR (film) 2977, 2094, 1690, 1241, 698 cm^{-1} ; HRMS (ESI⁺) calculated for $\text{C}_{18}\text{H}_{24}\text{N}_5\text{O}_2\text{S}$ [M+H] 374.1651, found 374.1613.

4.3.7. *Tert*-butyl *N*-{[4-(aminomethyl)-5-methyl-1,3-thiazol-2-yl]methyl}-*N*-benzylcarbamate (21)

Azide **20** (1.10 g, 2.95 mmol) was added to a 250 mL pressure flask with stir bar followed by methanol (70 mL). The flask was purged with argon, then 10% Pd/C (0.470 g, 0.442 mmol) was added. The reaction flask was attached to a Parr hydrogenator, evacuated, and backfilled with hydrogen to 2 atm x 3. The reaction was stirred vigorously under 2 atm of hydrogen for 3 h. A sample aliquot was taken from the reaction, dissolved in 1 mL HPLC grade MeCN, and analyzed with LC-MS to confirm reaction completion. The reaction mixture was passed through a pad of Celite, then concentrated to afford the title compound as a yellow oil (0.955 g, 93%). The crude product was used directly without further purification. TLC R_f = 0.39 (80:20 hexane:EtOAc); ^1H NMR (300 MHz, CDCl_3) δ = 1.51 (s, 9 H), 1.78 (br. s. 2 H), 2.37 (s, 3 H), 3.78 (s, 2 H), 4.38–4.67 (m, 4 H), 7.14–7.39 (m, 5 H); ^{13}C NMR (75 MHz, CDCl_3) δ = 11.2, 28.6, 39.5, 47.9, 50.0, 50.1, 50.8, 80.9, 127.6, 127.7, 128.4, 128.7, 137.7, 137.8, 151.8, 155.4, 155.7, 164.79; IR (film) 3054, 2976, 1691, 1452, 1117, 692 cm^{-1} ; HRMS (ESI⁺) calculated for $\text{C}_{18}\text{H}_{25}\text{N}_3\text{O}_2\text{S}$ [M+H] 348.1746, found 348.1701.

4.3.8. ({2-[(Benzylamino)methyl]-5-methyl-1,3-thiazol-4-yl}methyl)[(quinolin-8-yl)methyl]amine (22a)

Amine **21** (0.200 g, 0.576 mmol) was added to an oven dried 20 mL vial with stir bar followed by glacial acetic acid (4.5 mL). Next, quinoline-8-carbaldehyde (0.105 g, 0.633 mmol) and sodium triacetoxyborohydride (0.146 g, 0.691 mmol) were added. The vial was purged with nitrogen and the reaction was stirred for 16 h. A sample aliquot was taken from the reaction, dissolved in 1 mL HPLC grade MeCN, and analyzed with LC-MS to confirm reaction completion. 1.0 N aq. NaOH was added until the pH was greater than 12. The aqueous solution was saturated with NaCl and extracted with EtOAc (3 × 50 mL). The combined organic layers were washed with brine, dried over sodium sulfate and condensed to give a dark red/brown oil. The oil was dissolved with DCM (10 mL) and Amberlyst[®] 15 ion exchange resin (2 g) was added. The crude was stirred with the resin for 12 h. A sample

aliquot was taken from the reaction, dissolved in 1 mL HPLC grade MeCN, and analyzed with LC-MS to confirm reaction the product had bound completely to the resin. The resin was filtered and washed with EtOAc (50 mL). The washed resin was placed in a 50 mL round bottom flask with 3.5 N ammonia in methanol (30 mL) and stirred for 3 h. The resin was filtered and washed with 3.5 N ammonia in MeOH until no further material eluted, as detected by TLC. The combined washes were condensed to give a brown oil, which was dissolved with minimal DCM and purified by flash chromatography (5 g SiO₂; 0–12% 0.5 N NH₄ in MeOH:DCM) to give the title compound as a dark red oil (168 mg, 75%). TLC R_f = 0.73 (90:10 MeOH:DCM); ¹H NMR (400 MHz, CDCl₃) δ = 2.41 (s, 3 H), 3.84 (s, 2 H), 3.94 (s, 2 H), 4.02 (s, 2 H), 4.60 (s, 2 H), 7.25–7.36 (m, 5 H), 7.41 (dd, J = 8.2, 4.3 Hz, 1 H), 7.51 (dd, J = 8.2, 7.0 Hz, 1 H), 7.76 (dd, J = 19.4, 7.6 Hz, 2 H), 8.10–8.22 (m, 1 H), 8.78–8.90 (m, 1 H); ¹³C NMR (75 MHz, CDCl₃) δ = 11.5, 46.7, 50.4, 50.6, 53.4, 121.3, 126.5, 127.3, 127.5, 128.4, 128.6, 128.7, 129.1, 129.4, 136.6, 137.3, 140.0, 147.0, 149.5, 149.7, 167.7; IR (film) 3304, 2921, 1498, 1452, 792, 699 cm⁻¹; HRMS (ESI⁺) calculated for C₂₃H₂₅N₄S [M+H] 389.1800, found 389.1759.

4.3.9. 2-[[[2-[(Benzylamino)methyl]-5-methyl-1,3-thiazol-4-yl)methyl]amino]methyl]phenol (22b)
Amine **21** (0.150 g, 0.432 mmol) was added to an oven dried 100 mL round bottom flask with stir bar followed by anhydrous THF (35 mL). Next, salicylaldehyde (0.063 g, 0.52 mmol) and sodium triacetoxymethylborohydride (0.137 g, 0.648 mmol) were added. The vial was sealed under nitrogen and stirred for 16 h. A sample aliquot was taken from the reaction, dissolved in 1 mL HPLC grade MeCN, and analyzed with LCMS to confirm reaction completion. The reaction was washed with saturated ammonium chloride and the aqueous layer extracted with EtOAc (2 × 20 mL). The combined organic layers were washed with brine, dried over sodium sulfate and condensed to give a yellow oil. The oil was dissolved with DCM (10 mL) and Amberlyst[®] 15 ion exchange resin (2 g) was added. The crude was stirred with the resin for 12 h. A sample aliquot was taken from the reaction, dissolved in 1 mL HPLC grade MeCN, and analyzed with LC-MS to confirm the product had bound completely to the resin. After stirring the resin was filtered and washed with EtOAc before being placed in a 50 mL round bottom flask with 3.5 N ammonia in methanol and stirred for 3 h. The resin washed with 3.5 N ammonia in MeOH until no further material could be seen coming off the resin by TLC. Combined washes were condensed to give a yellow oil. The compound was purified by flash chromatography (12 g C18 cartridge; 15–95% MeOH:H₂O gradient) to afford the title compound as a pale yellow oil (70 mg, 45%). TLC R_f = 0.53 (90:10 DCM:MeOH); ¹H NMR (400 MHz, CDCl₃) δ = 2.30 (s, 3 H), 3.76 (s, 2 H), 3.87 (s, 2 H), 3.94 (s, 2 H), 4.03 (s, 2 H), 6.77 (t, J = 1.0 Hz, 1 H), 6.84 (d, J = 8.2 Hz, 1 H), 6.95 (d, J = 7.4 Hz, 1 H), 7.17 (t, J = 7.6 Hz, 1 H), 7.22–7.30 (m, 1 H), 7.30–7.41 (m, 4 H); ¹³C NMR (101 MHz, CDCl₃) δ = 11.1, 44.9, 50.2, 51.4, 53.2, 116.4, 119.0, 122.2, 127.2, 128.2, 128.5, 128.6, 128.7, 129.5, 139.7, 148.3, 158.3, 168.10; IR (film) 3322, 2973, 2921, 1455, 1256, 1044, 754, 657 cm⁻¹; HRMS (ESI⁺) calculated for C₂₀H₂₄N₃OS [M+H] 354.1640, found 354.1600.

4.3.10. 2-[[[2-[(Benzylamino)methyl]-5-methyl-1,3-thiazol-4-yl)methyl]amino]methyl]-4-chlorophenol (22c)

Prepared as described for **22b**. Purified by flash chromatography (5 g SiO₂ cartridge; 0–12% 0.5 N NH₄ in MeOH:DCM gradient) then (12 g C18 cartridge; 15–95% MeOH:H₂O gradient) to afford the title compound as a pale yellow oil (56 mg, 33%). TLC R_f = 0.50 (90:10 DCM:MeOH); ¹H NMR (400 MHz, CDCl₃) δ = 2.30 (s, 3 H), 3.75 (s, 2 H), 3.88 (s, 2 H), 3.92 (s, 2 H), 4.04 (s, 2 H), 6.68–6.80 (m, 1 H), 6.81–6.92 (m, 2 H), 7.18–7.43 (m, 5 H); ¹³C NMR (75 MHz, CDCl₃) δ = 11.3, 45.0, 50.4, 51.1, 53.5, 117.0, 119.3, 120.9, 127.5, 128.4, 128.7, 123.0, 129.8, 134.2, 139.8, 148.2, 159.5, 168.7; IR (film) 2952, 2865, 1479, 1236, 698 cm⁻¹; HRMS (ESI⁺) calculated for C₂₀H₂₃ClN₃OS [M+H] 388.1250, found 388.1241.

4.3.11. 2-[[[2-[(Benzylamino)methyl]-5-methyl-1,3-thiazol-4-yl)methyl]amino]methyl]-4,6-di-*tert*-butylphenol (22d)

Prepared as described for **22b**. Purified by flash chromatography (12 g C18 cartridge; 25–95% MeOH:H₂O gradient) to afford the desired product as a light brown oil (94 mg, 47%). TLC R_f = 0.66 (90:10 DCM:MeOH); ¹H NMR (400 MHz, CDCl₃) δ = 1.27 (s, 9 H), 1.42 (s, 9 H), 2.31 (s, 3 H), 3.76 (s, 2 H), 3.88 (s, 2 H), 3.92 (s, 2 H), 4.03 (s,

2 H), 6.81 (d, $J = 2.4$ Hz, 1 H), 7.22 (d, $J = 2.4$ Hz, 1 H), 7.23–7.39 (m, 5 H); ^{13}C NMR (101 MHz, CDCl_3) $\delta = 11.1, 30.0, 31.7, 34.1, 34.9, 44.9, 50.2, 52.3, 53.2, 121.5, 122.9, 123.5, 127.2, 128.2, 128.5, 129.4, 135.8, 139.6, 140.3, 148.5, 154.7, 168.10$; IR (film) 2920, 2843, 1604, 1488, 903, 699 cm^{-1} ; HRMS (ESI⁺) calculated for $\text{C}_{28}\text{H}_{40}\text{N}_3\text{OS}$ [M+H] 466.2892, found 466.2863.

4.3.12. *Tert*-butyl 2-[[*(2S,3R)*-3-hydroxy-1-methoxy-1-oxobutan-2-yl]carbamoyl]pyrrolidine-1-carboxylate (23)

N-Boc-L-proline (**14**) (5.38 g, 24.5 mmol) and L-threonine methyl ester, HCl salt (**13**) (4.16 g, 24.5 mmol) were added to a 1.0 L round bottom flask with stir bar containing DCM (400 mL). HOBt (4.13 g, 27.0 mmol) was added followed by TEA (8.60 mL, 61.7 mmol) and EDC HCl (5.17 g, 27.0 mmol). The reaction was stirred for 20 h. A sample aliquot was taken from the reaction, dissolved in 1 mL HPLC grade MeCN, and analyzed with LC-MS to confirm reaction completion. The reaction was washed with half saturated aq. sodium bicarbonate (2 × 200 mL) and 0.2 N HCl (2 × 200 mL). The combined aqueous washes were extracted with DCM (2 × 100 mL). The combined organics were washed with brine, dried over sodium sulfate, filtered, and condensed to give the title compound as a colorless oil (5.91 g, 73%). The crude product was pushed forward without further purification. This compound has been previously reported and characterized (CAS# 80897-23-0). ^1H NMR (300 MHz, CDCl_3) $\delta = 1.19$ (d, $J = 6.4$ Hz, 3H), 1.47 (s, 9H), 1.80–2.35 (m, 4H), 3.39–3.48 (m, 2H), 3.77 (d, $J = 1.7$ Hz, 3H), 4.26–4.36 (m, 2H), 4.58 (dd, $J = 9.0, 2.6$ Hz, 1H).

4.3.13. *Tert*-butyl 2-[[*(2S)*-1-methoxy-1,3-dioxobutan-2-yl]carbamoyl]pyrrolidine-1-carboxylate (24)

Alcohol **23** (5.91 g, 17.9 mmol) was added to a 1 L round bottom flask with stir bar followed by DCM (300 mL) and Dess-Martin periodinane (8.35 g, 19.7 mmol). The flask was sealed with a septum and flushed with nitrogen. The reaction was stirred for 3 h before water (0.322 mL, 17.9 mmol) was added and the reaction stirred for another 3 h. A sample aliquot was taken from the reaction, dissolved in 1 mL HPLC grade MeCN, and analyzed with LC-MS to confirm reaction completion. The reaction was poured on to a 10% sodium thiosulfate solution (400 mL) and stirred for 45 min until both layers turned clear. The organic layer was separated, washed with saturated aq. sodium bicarbonate (2 × 100 mL) and brine, then dried over sodium sulfate, filtered, and condensed to give a yellow oil. The crude was purified by flash chromatography (100 g SiO_2 cartridge; 0–80% EtOAc/hexanes gradient) to yield the title compound as a yellow oil (4.60 g, 78%). This compound has been previously reported and characterized (CAS# 1027049-00-8).

4.3.14. Methyl 2-[1-[(*tert*-butoxy)carbonyl]pyrrolidin-2-yl]-5-methyl-1,3-thiazole-4-carboxylate (25)

Ketone **24** (4.59 g, 14.0 mmol) was added to a 250 mL round bottom flask with stir bar followed by anhydrous THF (150 mL). The headspace was purged with nitrogen, then Lawesson's Reagent (8.46 g, 20.9 mmol) was added. The flask was fitted with a reflux condenser and the apparatus sealed with a septum and purged with nitrogen for 15 min, before being heated to reflux for 18 h. A sample aliquot was taken from the reaction, dissolved in 1 mL HPLC grade MeCN, and analyzed with LC-MS to confirm reaction completion. The reaction was condensed to an oil, then dissolved in EtOAc (250 mL) and washed with saturated aq. sodium bicarbonate (2 × 250 mL). The aqueous washes were extracted with EtOAc (100 mL), and the combined organics were washed with brine, dried over sodium sulfate, filtered, and condensed to give a red oil. The oil was adsorbed onto SiO_2 (25 g), then purified by flash chromatography (100 g SiO_2 cartridge; 0–40% EtOAc/hexanes gradient) to yield the title compound as an orange oil (3.46 g, 76%). This compound has been previously reported and characterized (CAS# 838853-22-8): ^1H NMR (300 MHz, CDCl_3) $\delta = 1.30$ –1.55 (m, 9H), 1.84–2.00 (m, 2H), 2.12–2.45 (m, 2H), 3.37–3.65 (m, 2H), 3.93 (s, 3H), 5.15 (d, $J = 13.8$ Hz, 1H).

4.3.15. *Tert*-butyl 2-[4-(hydroxymethyl)-5-methyl-1,3-thiazol-2-yl]pyrrolidine-1-carboxylate (26)

Ester **25** (3.43 g, 10.5 mmol) was added to an oven dried 100 mL round bottom flask followed by sodium triacetoxyborohydride (0.112 g, 0.525 mmol), and sodium borohydride (0.898 g, 23.1 mmol). The flask was fitted with a septum and the headspace purged with nitrogen before anhydrous THF (30 mL) was added via cannula.

The reaction stirred for 5 min then anhydrous methanol (1.70 mL, 42.0 mmol) was added via syringe over 15 min. The reaction was heated to 35 °C for 16 h. A sample aliquot was taken from the reaction, dissolved in 1 mL HPLC grade MeCN, and analyzed with LC-MS to confirm reaction completion. The reaction was diluted with EtOAc (30 mL) and quenched with saturated aq. ammonium chloride. The layers were separated and the aqueous layer was extracted with 10% MeOH in DCM (3 × 50 mL). The combined organic layers were washed with brine and condensed to give a thick yellow oil (2.65 g, 85%). The crude material was moved forward without purification. [a]_{D25} -78.36 (0.573, DCM); TLC R_f: 0.57 (90:10 DCM:MeOH); ¹H NMR (300 MHz, CDCl₃) δ = 1.34–1.47 (m, 9H), 1.89–1.94 (m, 2H), 2.17–2.28 (m, 1H), 2.37–2.40 (m, 2H), 3.39–3.56 (m, 2H), 4.62 (s, 3H), 5.03–5.15 (m, 1H); ¹³C NMR is complicated due to rotamers. ¹³C NMR (75 MHz, CDCl₃) δ = 11.1, 23.2, 24.0, 28.4, 28.5, 32.9, 34.1, 46.6, 47.0, 58.1, 58.9, 59.4, 80.2, 128.5, 128.7, 150.7, 150.8, 154.4, 154.8, 171.5, 172.35; IR (film) 3377, 2975, 1698, 1388, 1366, 1165, 770 cm⁻¹; HRMS (ESI⁺) calcd for C₁₄H₂₂N₂O₃S [M+H]⁺ 299.1424, found 299.1405.

4.3.16. *Tert*-butyl 2-[4-(azidomethyl)-5-methyl-1,3-thiazol-2-yl]pyrrolidine-1-carboxylate (27)

Alcohol **26** (2.12 g, 7.11 mmol) was added to an oven dried 250 mL round bottom flask. The flask was purged with nitrogen and anhydrous DCM (50 mL) was added followed by mesyl chloride (0.660 mL, 8.53 mmol) and triethylamine (1.12 mL, 8.61 mmol). The reaction was stirred at room temperature for 24 h. A sample aliquot was taken from the reaction, dissolved in 1 mL HPLC grade MeCN, and analyzed with LC-MS to confirm reaction completion. The DCM was evaporated and the crude oil dissolved with anhydrous DMF (50 mL). Sodium azide (0.544 g, 8.53 mmol) was added in one portion and the reaction stirred for 16 h. The reaction was diluted with ether (250 mL) and washed with water (3 × 250 mL). The aqueous layers were extracted with ether (2 × 100 mL). The combined organics were washed with brine, dried over sodium sulfate, filtered, and condensed to give an orange oil. The oil was dissolved with minimal DCM and purified by flash chromatography (25 g SiO₂ cartridge; 0–20% EtOAc:hexanes gradient) to give the title compound as a yellow oil (1.73 g, 75%). [a]_{D25} -86.52 (0.620, DCM); TLC R_f = 0.40 (80:20 hexane:EtOAc); ¹H NMR (300 MHz, CDCl₃) δ = 1.36–1.48 (m, 9H), 1.92–1.94 (m, 2H), 2.21–2.26 (m, 2H), 2.42 (s, 3H), 3.44–3.55 (m, 2H), 4.33 (s, 2H), 5.03–5.12 (m, 1H); ¹³C NMR is complicated due to rotamers. ¹³C NMR (100 MHz, CDCl₃) δ = 11.2, 23.1, 23.9, 28.3, 28.4, 32.5, 33.8, 46.5, 46.9, 47.5, 58.8, 59.3, 80.0, 80.1, 130.8, 131.0, 145.7, 146.0, 154.2, 154.6, 171.2, 172.3; IR (film) 2976, 2093, 1695, 1384, 1166, 1113, 769 cm⁻¹; HRMS (ESI⁺) calcd for C₁₄H₂₁N₅O₂S [M+H]⁺ 324.1489, found 324.1457.

4.3.17. *Tert*-butyl 2-[4-(aminomethyl)-5-methyl-1,3-thiazol-2-yl]pyrrolidine-1-carboxylate (28)

Azide **27** (1.63 g, 5.05 mmol) was added to a 250 mL pressure flask followed by methanol (50 mL). The flask was purged with argon then 10% Pd/C (0.537 g, 0.505 mmol) was added. The reaction flask was attached to a Parr hydrogenator, evacuated, and backfilled with hydrogen x 3. The reaction was stirred vigorously under 3 bar of hydrogen for 16 h. A sample aliquot was taken from the reaction, dissolved in 1 mL HPLC grade MeCN, and analyzed with LCMS to confirm reaction completion. The reaction mixture was passed through a pad of Celite, then concentrated to afford a colorless oil (1.30 g, 87%). The crude product was used directly without further purification. [a]_{D25} -83.71 (0.653, DCM); TLC R_f: 0.39 (90:10 DCM:MeOH); ¹H NMR (300 MHz, CDCl₃) δ = 1.35–1.49 (m, 9H), 1.67 (br. s, 2H), 1.92–1.95 (m, 2H), 2.21–2.28 (m, 2H), 2.37 (s, 3H), 3.39–3.57 (m, 3H), 3.79 (s, 2H), 5.01–5.15 (m, 1H); ¹³C NMR is complicated due to rotamers. ¹³C NMR (100 MHz, CDCl₃) δ = 11.1, 23.2, 23.9, 28.4, 28.6, 32.9, 34.0, 39.8, 46.5, 47.0, 59.0, 59.5, 80.1, 126.5, 126.6, 152.5, 152.8, 154.4, 154.8, 171.1, 171.72; IR (film) 3356, 3301, 2974, 1694, 1385, 1164, 1113, 770 cm⁻¹; HRMS (ESI⁺) calcd for C₁₄H₂₃N₃O₂S [M+H]⁺ 298.1584, found 298.1548.

4.3.18. {[5-Methyl-2-(pyrrolidin-2-yl)-1,3-thiazol-4-yl]methyl}[(quinolin-8-yl)methyl]amine (29a)

Amine **28** (0.200 g, 0.576 mmol) was added to an oven dried 25 mL vial with stir bar followed by glacial acetic acid (5.0 mL). Next, quinoline-8-carbaldehyde (0.128 g, 0.777 mmol) and sodium triacetoxyborohydride (0.180, 0.847 mmol) were added. The vial was purged with nitrogen and allowed to stir for 16 h. A sample aliquot was taken from the reaction, dissolved in 1 mL HPLC grade MeCN, and analyzed with LCMS to confirm reaction

completion. The reaction was neutralized with saturated aq. sodium bicarbonate and brought to pH = 9. The aqueous solution was extracted with EtOAc (2 × 20 mL). The combined organic layers were washed with brine, dried over sodium sulfate, filtered, and condensed to give a dark orange oil. The oil was dissolved with DCM (50 mL), and Amberlyst® 15 ion exchange resin (4 g) was added. The crude was stirred with the resin for 16 h. A sample aliquot was taken from the reaction, dissolved in 1 mL HPLC grade MeCN, and analyzed with LC-MS to confirm that the desired product had completely bound to the resin. The resin was filtered and washed with DCM (50 mL) and MeOH (50 mL). The washed resin was placed in a 50 mL round bottom flask with 3.5 N ammonia in methanol (30 mL) and was stirred for 16 h. After 16 h, the resin was filtered and washed with 3.5 N ammonia in MeOH until no further material was eluted, as detected by TLC. The combined washes were condensed to give a yellow oil. The crude was purified by flash chromatography (5 g SiO₂; 0–27% 0.5N NH₃ in MeOH:DCM) to give the title compound as a pale yellow oil (75 mg, 32%). [α]_{D25} -37.73 (0.273, DCM); TLC R_f = 0.16 (90:10 MeOH:DCM); ¹H NMR (400 MHz, CDCl₃) δ = 1.72–1.99 (m, 3H), 2.18–2.29 (m, 1H), 2.32 (s, 3H), 2.53 (br s, 2H), 3.01 (ddd, *J* = 10.0, 7.6, 6.5 Hz, 1H), 3.10 (ddd, *J* = 10.0, 7.2, 5.3, 1H), 3.85 (s, 2H), 4.39–4.49 (m, 3H), 7.40 (dd, *J* = 8.3, 4.2 Hz, 1H), 7.49 (dd, *J* = 8.3, 6.9 Hz, 1H), 7.67–7.75 (m, 2H), 8.14 (dd, *J* = 8.3, 1.8 Hz, 1H), 8.91 (dd, *J* = 4.2, 1.8 Hz, 1H); ¹³C NMR (100 MHz, CDCl₃) δ = 11.3, 25.6, 33.9, 47.0, 50.4, 49.9, 121.0, 126.4, 127.0, 127.9, 128.4, 128.9, 136.40, 138.4, 147.0, 149.5, 150.4, 173.7; IR (film) 3301, 2919, 1498, 1445, 828, 792 cm⁻¹; HRMS (ESI⁺) calcd for C₁₉H₂₂N₄S [M+H]⁺ 339.1638, found 339.1607.

4.3.19. 2-[[[5-Methyl-2-(pyrrolidin-2-yl)-1,3-thiazol-4-yl]methyl]amino)methyl]phenol (29b)

Amine **28** (0.195 g, 0.655 mmol) was added to an oven dried 100 mL round bottom flask followed by anhydrous THF (30 mL). Next, salicylaldehyde (0.088 g, 0.720 mmol) and sodium triacetoxyborohydride (0.167 g, 0.786 mmol) were added. The vial was purged with nitrogen and stirred for 16 h. A sample aliquot was taken from the reaction, dissolved in 1 mL HPLC grade MeCN, and analyzed with LC-MS to confirm reaction completion. Next, the reaction was quenched with saturated aq. ammonium chloride and basified with saturated aq. sodium bicarbonate. The aqueous layer was extracted with EtOAc (2 × 20 mL) and the combined organic layers were washed with brine, dried over sodium sulfate, filtered, and condensed to give a yellow oil. The oil was dissolved with DCM (50 mL), and Amberlyst® 15 ion exchange resin (4 g) was added. The crude was stirred with the resin for 16 h. A sample aliquot was taken from the reaction, dissolved in 1 mL HPLC grade MeCN, and analyzed with LC-MS to confirm that the desired product had completely bound to the resin. The resin was filtered and washed with DCM (50 mL) and MeOH (50 mL). The washed resin was placed in a 50 mL round bottom flask with 3.5 N ammonia in methanol (30 mL) and was stirred for 16 h. After 16 h, the resin was filtered and washed with 3.5 N ammonia in MeOH until no further material was eluted, as determined by TLC. The combined washes were condensed to give a brown oil. The compound was purified by flash chromatography (10 g SiO₂; 0–12% 0.5N NH₃ in MeOH:DCM) to afford a colorless oil (119 mg, 60%). [α]_{D25} -45.04 (2.280, DCM); TLC R_f = 0.19 (90:10 DCM:MeOH); ¹H NMR (400 MHz, CDCl₃) δ = 1.74–1.98 (m, 3H), 2.22–2.26 (m, 4H), 2.97–3.17 (m, 2H), 3.74 (s, 2H), 3.93 (s, 2H), 4.45 (dd, *J* = 8.0, 5.4 Hz, 1H), 6.76 (td, *J* = 7.4, 1.2 Hz, 1H), 6.83 (dd, *J* = 8.1, 1.1 Hz, 1H), 6.94 (dd, *J* = 7.4, 1.5 Hz, 1H), 7.16 (td, *J* = 8.0, 1.7 Hz, 1H); ¹³C NMR (100 MHz, CDCl₃) δ = 11.0, 25.6, 33.9, 45.0, 47.0, 51.4, 49.8, 116.4, 119.0, 122.3, 128.6, 128.7, 128.9, 148.4, 158.3, 174.8; IR (film) 3290, 2920, 1589, 1490, 1474, 1456, 1256, 754 cm⁻¹; HRMS (ESI⁺) calcd for C₁₆H₂₁N₃OS [M+H]⁺ 304.1478, found 304.1452.

4.3.20. 4-Chloro-2-[[[5-methyl-2-(pyrrolidin-2-yl)-1,3-thiazol-4-yl]methyl]amino)methyl]phenol (29c)

Prepared as described for **29b**. Compound purified by flash chromatography (10 g SiO₂; 0–12% 0.5N NH₄ in MeOH:DCM) to afford the title compound as a yellow oil (101 mg, 43%). [α]_{D25} -39.46 (0.147, DCM); TLC R_f = 0.33 (90:10 DCM:MeOH); ¹H NMR (400 MHz, CDCl₃) δ = 1.81–1.99 (m, 3H), 2.21–2.27 (m, 4H), 2.99–3.19 (m, 2H), 3.73 (s, 2H), 3.90 (s, 2H), 4.47 (dd, *J* = 7.6, 5.4 Hz, 1H), 5.52 (br s, 2H), 6.73 (dd, *J* = 8.0, 2.0 Hz, 1H), 6.81–6.87 (m, 2H); ¹³C NMR (100 MHz, CDCl₃) δ = 11.1, 25.5, 33.9, 44.8, 46.9, 50.8, 59.7, 116.7, 119.0, 120.8, 129.2, 129.4, 133.9, 148.0, 159.2, 174.1; IR (film) 2923, 1585, 1447, 1237, 1081, 902 cm⁻¹; HRMS (ESI⁺) calcd for C₁₆H₂₀N₃OSCl [M+H]⁺ 338.1088, found 338.1058.

4.3.21. 2,4-Di-*tert*-butyl-6-[[[5-methyl-2-(pyrrolidin-2-yl)-1,3-thiazol-4-yl]methyl]amino)methyl]phenol (29d)

Prepared as described for **29b**. Compound purified by flash chromatography (10 g SiO₂; 0–7% 0.5N NH₄ in MeOH:DCM) to afford the title compound as a colorless oil (91 mg, 48%). [α]_D25 -30.41 (1.207, DCM); TLC R_f = 0.48 (90:10 DCM:MeOH); ¹H NMR (300 MHz, CDCl₃) δ = 1.28 (s, 9H), 1.42 (s, 9H), 1.90 (m, 3H), 2.20–2.28 (m, 4H), 3.01–3.17 (m, 2H), 3.75 (s, 2H), 3.91 (s, 2H), 4.46 (dd, *J* = 7.7, 5.4 Hz, 2H), 6.82 (d, *J* = 1.8 Hz, 1H), 7.22 (d, *J* = 1.8 Hz, 1H); ¹³C NMR (75 MHz, CDCl₃) δ = 11.2, 25.6, 29.7, 31.8, 34.0, 34.2, 35.0, 45.1, 47.0, 52.4, 59.7, 121.7, 123.0, 123.6, 128.9, 135.9, 140.4, 148.7, 154.8, 174.5; IR (film) 3276, 2951, 1480, 1485, 1443, 1236, 877, 820 cm⁻¹; HRMS (ESI⁺) calcd for C₂₄H₃₇N₃OS [M+H]⁺ 416.2730, found 416.2709.

4.4. General protocol for intramolecular carbocyclization screens

The procedure used was adopted from the protocol reported by Michelet [28]. First, a stock solution was made by adding formyl alkyne **1a** (200 mg, 0.790 mmol) and cyclohexylamine (0.018 mL, 0.16 mmol) to a 4 mL vial with stir bar containing DCE (2.0 mL). After 10 min, 0.2 mL of this solution which contained formyl alkyne **1a** (0.020 g, 0.079 mmol) and cyclohexylamine (1.8 μL, 0.016 mmol), was added to a 1.5 mL HPLC vial, which contained a solution of the ligand (0.012 mmol) and metal salt (0.012 mmol) in DCE (0.15 mL). The vials were capped and shaken for 16 h. The reaction mixtures were filtered through silica plugs in Pasteur pipets, eluted with EtOAc (~2 mL), and condensed. Yields of **1b** were measured by ¹H NMR in CDCl₃ using pentachloroethane as an internal standard. Reactions using Cu(I) metal salts followed the same general procedure, however sample vials were set up in the glovebox and stirred on the benchtop.

4.5. General procedure for intermolecular reaction screens

First, alkyne and carbonyl stock solutions were made by mixing the alkyne (0.65 mmol) with DCE (0.75 mL) in a 1.5 mL HPLC vial. Carbonyl compounds (0.155 mmol) were mixed with DCE (0.6 mL) in a 1.5 mL HPLC vial. The vials were sealed and argon was bubbled through the solutions for 10 min before they were brought into the glovebox. In the glovebox, ligand **22a** and (CH₃CN)₄CuBF₄ stock solutions was made by weighing the metal salt (0.035 g, 0.109 mmol) into a 20 mL scintillation vial, followed by addition of **22a** (0.042 g, 0.109 mmol) as a solution in 10.5 mL DCE. 0.5 mL of this stock solution containing **22a** (2.0 mg, 0.005 mmol) and (CH₃CN)₄CuBF₄ (1.7 mg 0.005 mmol) was added to separate HPLC vials before the alkyne (0.130 mmol) was added as a stock solution (0.15 mL to each vial), followed by the stock solution of carbonyl compound (0.10 mL, 0.026 mmol). If additives (0.005 mmol) were used, they were added at this point as solutions in 0.1 mL DCE. The reaction vials were removed from the glovebox, sealed with parafilm, and heated in a sand bath at 50 °C without stirring for 16 h. After heating, the samples were directly analyzed by GC-MS. GC-MS method (see General Information for further details): 50 °C–100 °C over 2 min, then hold at 100 °C for 2 min, ramp to 280 °C over 18 min, then hold at 280 °C for 8 min 2 μL injection volume.

4.6. General protocol for crystallizations of metal complexes

In the glovebox, Cu(I) metal salts (0.010 mmol) were weighed into an oven dried 1.5 mL HPLC vial. The ligand (0.010 mmol) was added to the metal salt as a solution in CH₃NO₂ (0.5 mL). The vial caps were pierced with a needle and the vials were sealed in a Chemglass Airfree[®] drying chamber. The chamber was removed from the glovebox and placed under vacuum (0.1 mm Hg) for 12 h to remove the solvent. The dried samples were brought back into the glovebox where they were dissolved with 0.1 mL 1:1 CH₃NO₂:benzene and placed in a shortened 5 mm NMR tube (~2.5 cm long), which was set inside of a 4 mL vial. Ether (0.4 mL) was added to the vial containing the sample tube, and the vials were tightly capped with septa, placed into the Chemglass Airfree[®] drying chamber, and removed from the glovebox. The chamber sat in a dark cabinet for 3–7 days to allow crystals to form. Samples containing non-oxygen sensitive complexes were set up outside of the glovebox but followed the same general procedure.

4.7. Crystallographic data

CCDC 1834245 and 1834246 (Fig. 3) and 1833343 (Fig. 4) contain the supplementary crystallographic data for this paper. These data can be obtained free of charge from the Cambridge Crystallographic Data Centre via <https://www.ccdc.cam.ac.uk>.

4.8. Protocol for NMR binding studies with precatalyst

Precatalyst **22a** (0.004 g, 0.010 mmol) was added to a 4 mL vial followed by CD₃NO₂ (0.8 mL). The vial was sealed with a septum and the solution was purged with argon for 10 min before being brought into the glovebox. (CH₃CN)₄CuBF₄ (0.003 g, 0.010 mmol) was weighed into a 1.5 mL HPLC vial in the glovebox, and the ligand solution was transferred to this vial. After the solution became homogeneous, 0.4 mL was transferred to an NMR tube for analysis. To the remainder of the solution in the glovebox, phenylacetylene (0.5 μL, 0.005 mmol) was added via microsyringe. This solution was transferred to an NMR tube for analysis.

Author contributions

Conceived project: C.D. Designed catalysts: C.D., J.D.P., A.R.B. Performed Conia-ene studies: J.D.P. Performed NMR studies: J.D.P. Performed DFT calculations: J.D.P., E.G., C.D. Synthesized and characterized precatalysts: J.D.P., E.G., A.A., A.R.B. Screened reactions: J.D.P., E.G. Performed crystallization studies: J.D.P. Performed x-ray diffraction and data analysis: S.L. Wrote the manuscript: C.D., J.D.P.

Notes

An earlier version of this manuscript was submitted to the preprint server ChemRxiv: <https://doi.org/10.26434/chemrxiv.6163430.v1>.

Acknowledgments

We thank Dr. Sheng Cai for assistance with LC-MS and NMR instruments, Prof. Chae Yi for helpful comments, Shimadzu Inc. for a grant to support the purchase of the LC-MS used in these studies, Marquette University for startup funding, and the American Chemical Society Petroleum Research Fund (grant number 55732-DNI1) for support of this project. We also thank ChemAxon and ACD/Labs for use of their NMR prediction and processing software.

Appendix A. Supplementary data

The following is the supplementary data related to this article:

Figure S1 (Comparison of DFT calculations of Cu(I) vs Ag(I) metals for bifunctional catalysis of C—C formation with acetone and acetylene); Table S1 (DFT calculations for bifunctional catalysis of C—C bond formation with acetone and 1-butyne); Figure S2 (Representative DFT-optimized structures of alkyne complex (**10**) and adduct after C—C bond formation (**11**)); Figure S3 (NMR study of Cu(I) complex); ¹H and ¹³C NMR spectra; representative Gaussian input files; Cartesian coordinates for select DFT-optimized structures.

Download Acrobat PDF file (4MB)Help with pdf files
Multimedia component 1.

Research data for this article

Cambridge Crystallographic Data Center

Crystallographic data

Data associated with the article:

CCDC 1834246: Experimental Crystal Structure Determination

CCDC 1833343: Experimental Crystal Structure Determination

CCDC 1834245: Experimental Crystal Structure Determination

About research data

References

- [1] B. List, R.A. Lerner, C.F. Barbas *J. Am. Chem. Soc.*, 122 (2000), pp. 2395-2396
- [2] R. Mahrwald *Drug Discov. Today Technol.*, 10 (2013), pp. e29-e36
- [3] A.E. Allen, D.W.C. MacMillan *Chem. Sci.*, 3 (2012), p. 633
- [4] Z. Du, Z. Shao *Chem. Soc. Rev.*, 42 (2013), p. 1337
- [5] Y. Deng, S. Kumar, H. Wang *Chem. Commun.*, 50 (2014), p. 4272
- [6] A. Gualandi, L. Mengozzi, C.M. Wilson, P.G. Cozzi *Chem. Asian J.*, 9 (2014), pp. 984-995
- [7] P.J. Walsh, M.C. Kozlowski **Fundamentals of Asymmetric Catalysis** University Science Books (2009)
- [8] Y. Ito, M. Sawamura, T. Hayashi *J. Am. Chem. Soc.*, 108 (1986), pp. 6405-6406
- [9] Y. Hamashima, D. Sawada, M. Kanai, M. Shibasaki *J. Am. Chem. Soc.*, 121 (1999), pp. 2641-2642
- [10] S. France, M.H. Shah, A. Weatherwax, H. Wack, J.P. Roth, T. Lectka *J. Am. Chem. Soc.*, 127 (2005), pp. 1206-1215
- [11] D. Wiedenhoef, A. Benoit, J. Porter, Y. Wu, R. Viridi, A. Shanaa, C. Dockendorff *Synthesis*, 48 (2016), pp. 2413-2422
- [12] D. Wiedenhoef, A.R. Benoit, Y. Wu, J.D. Porter, E. Meyle, T.H.W. Yeung, R. Huff, S.V. Lindeman, C. Dockendorff *Tetrahedron*, 72 (2016), pp. 3905-3916
- [13] J. Paradowska, M. Pasternak, B. Gut, B. Gryzł, J. Mlynarski *J. Org. Chem.*, 77 (2012), pp. 173-187
- [14] M. Pasternak, J. Paradowska, M. Rogozińska, J. Mlynarski *Tetrahedron Lett.*, 51 (2010), pp. 4088-4090
- [15] J. Paradowska, M. Stodulski, J. Mlynarski *Adv. Synth. Catal.*, 349 (2007), pp. 1041-1046
- [16] Z. Xu, P. Daka, H. Wang *Chem. Commun.* (2009), p. 6825
- [17] Z. Xu, P. Daka, I. Budik, H. Wang, F.-Q. Bai, H.-X. Zhang *Eur. J. Org. Chem.*, 2009 (2009), pp. 4581-4585
- [18] P. Daka, Z. Xu, A. Alexa, H. Wang *Chem. Commun.*, 47 (2011), pp. 224-226
- [19] T. Pei, R.A. Widenhofer *J. Am. Chem. Soc.*, 123 (2001), pp. 11290-11291
- [20] X. Wang, R.A. Widenhofer *Chem. Commun.* (2004), pp. 660-661
- [21] D. Hack, M. Blumel, P. Chauhan, A.R. Philipps, D. Enders *Chem. Soc. Rev.*, 44 (2015), pp. 6059-6093
- [22] J.T. Binder, B. Crone, T.T. Haug, H. Menz, S.F. Kirsch *Org. Lett.*, 10 (2008), pp. 1025-1028
- [23] T. Yang, A. Ferrali, L. Campbell, D. Dixon *J. Chem. Commun.* (2008), p. 2923
- [24] K.L. Jensen, P.T. Franke, C. Arróniz, S. Kobbelgaard, K.A. Jørgensen *Chem. Eur. J.*, 16 (2010), pp. 1750-1753
- [25] Y.-P. Xiao, X.-Y. Liu, C.-M. Che *Angew. Chem. Int. Ed.*, 50 (2011), pp. 4937-4941
- [26] B. Montaignac, M.R. Vitale, V. Michelet, V. Ratovelomanana-Vidal *Org. Lett.*, 12 (2010), pp. 2582-2585
- [27] B. Montaignac, M.R. Vitale, V. Ratovelomanana-Vidal, V. Michelet *J. Org. Chem.*, 75 (2010), pp. 8322-8325
- [28] B. Montaignac, M.R. Vitale, V. Ratovelomanana-Vidal, V. Michelet *Eur. J. Org. Chem.*, 2011 (2011), pp. 3723-3727
- [29] B. Montaignac, C. Praveen, M.R. Vitale, V. Michelet, V. Ratovelomanana-Vidal *Chem. Commun.*, 48 (2012), pp. 6559-6561
- [30] K. Endo, T. Hatakeyama, M. Nakamura, E. Nakamura *J. Am. Chem. Soc.*, 129 (2007), pp. 5264-5271
- [31] T. Fujimoto, K. Endo, H. Tsuji, M. Nakamura, E. Nakamura *J. Am. Chem. Soc.*, 130 (2008), pp. 4492-4496
- [32] F. Mo, G. Dong *Science*, 345 (2014), pp. 68-72
- [33] Z. Wang, B.J. Reinius, G. Dong *Chem. Commun.*, 50 (2014), p. 5230
- [34] F. Mo, H.N. Lim, G. Dong *J. Am. Chem. Soc.*, 137 (2015), pp. 15518-15527
- [35] T. Ankner, C.C. Cosner, P. Helquist *Chem. Eur. J.*, 19 (2013), pp. 1858-1871
- [36] J.M. Stevens, D.W.C. MacMillan *J. Am. Chem. Soc.*, 135 (2013), pp. 11756-11759

- [37] D.J. Berrisford, C. Bolm, K.B. Sharpless *Angew. Chem. Int. Ed.*, 34 (1995), pp. 1059-1070
- [38] C.E. Meyet, C.J. Pierce, C.H. Larsen *Org. Lett.*, 14 (2012), pp. 964-967
- [39] X. Tang, J. Kuang, S. Ma *Chem. Commun.*, 49 (2013) 8976–3
- [40] A. Becke *Phys. Rev. A Gen. Phys.*, 38 (1988), pp. 3098-3100
- [41] P.J. Hay, W.R. Wadt *J. Chem. Phys.*, 82 (1985), pp. 270-283
- [42] R.A. Kendall, T.H. Dunning Jr., R.J. Harrison *J. Chem. Phys.*, 96 (1992), pp. 6796-6806
- [43] M.G. Evans, M. Polanyi *Trans. Faraday Soc.*, 31 (1935), pp. 875-894
- [44] I. Thomsen, U. Pedersen, P.B. Rasmussen, B. Yde, T.P. Andersen, S.O. Lawesson *Chem. Lett.* (1983), pp. 809-810
- [45] G. Stork, A. Brizzolara, H. Landesman, J. Szmuszkovicz, R. Terrell *J. Am. Chem. Soc.*, 85 (1963), pp. 207-222
- [46] D. Sánchez, D. Bastida, J. Burés, C. Isart, O. Pineda, J. Vilarrasa *Org. Lett.*, 14 (2012), pp. 536-539
- [47] B.A. Trofimov, E.Y. Schmidt, N.V. Zorina, E.V. Ivanova, I.A. Ushakov *J. Org. Chem.*, 77 (2012), pp. 6880-6886
- [48] M.D. Hanwell, D.E. Curtis, D.C. Lonie, T. Vandermeersch, E. Zurek, G.R. Hutchison *J. Cheminf.*, 4 (2012), p. 17